Experimental investigation of the emission of high-energy particles in reactions with heavy ions at energies up to 10 MeV/nucleon

Yu. É. Penionzhkevich, E. Gierlik, V. V. Kamanin, and C. Borcea

Joint Institute for Nuclear Research, Dubna

Fiz. Elem. Chastits At. Yadra **17**, 165–223 (March–April 1986)

The main characteristics of processes involving the emission of high-energy particles—the total cross section for their production, the energy spectra, and the angular distributions—are considered. The emission of high-energy neutrons is compared with the emission of charged particles. A study is made of the distribution of the angular momenta between the products of reactions accompanied by the emission of high-energy particles, and also of the possibility of determining the spins of the residual nuclei. The correlations of the high-energy particles with the other reaction products are considered. Some applications of reactions with the emission of high-energy particles for obtaining and studying the properties of exotic nuclei are discussed. The main theoretical approaches to the explanation of the emission of high-energy particles are briefly described.

INTRODUCTION

The study of the emission of high-energy charged particles and neutrons in heavy-ion reactions has considerable independent interest. This is explained both by the unusual production mechanism of these particles and by the possibilities that these as yet little studied processes open up for obtaining nuclei with different properties (heavy and superheavy weakly excited nuclei, rapidly rotating nuclei, nuclei with large deformation, etc.).

It is well known that the strongly inelastic interaction of two complex nuclei, characterized by significant changes of the nucleon composition in the exit channel of the reaction, is, as a rule, associated with redistribution of the kinetic energy between the internal degrees of freedom of the nuclei that are formed. The limiting case of this process is the formation of a compound nucleus with a lifetime exceeding by several orders of magnitude the characteristic time of the internuclear motion of the nucleons ($\tau_n \sim 10^{-23}$ sec). Some general features of the decay of the system that is formed can be well described in the framework of statistical theory. However, it was noted long ago that it is not possible in the framework of statistical models to describe all the measurable experimental characteristics of compound-nucleus decay. The discrepancy between the statistical calculations and the experimental values increases with increasing energy of the bombarding ions. As an illustration of this we can take the excitation function for the reaction ^{176}Lu(^{22}Ne, αxn)$^{194-x}$Au shown in Fig. 1. It can be seen that in the region of high excitation energies there is a significant difference between the experimental excitation function and the one calculated by the statistical model. This difference is due to the production of α particles with cross sections and energies appreciably greater than those expected on the basis of the evaporation decay model of the compound nucleus.

More than 20 years ago measurements of the energy spectra of the protons and α particles produced in reactions with accelerated ^{12}C and ^{14}N ions on a ^{197}Au target enabled Britt and Quinton[1] to show that two components can be identified in the energy spectra of the α particles. One is due to the evaporation of α particles from the compound nucleus. The spectrum of these α particles has the form $N(E_\alpha) \sim E_\alpha \sigma_c(E_\alpha)\exp(-E_\alpha/T)$, where T is the temperature of the nucleus, and the angular distribution is symmetric with respect to 90° in the center-of-mass system. The second, harder component in the α-particle energy spectrum had an angular distribution directed forward and a velocity spectrum of the form $P(v) \sim v^2 \exp(-v^2/v_0^2)$ with a maximum of the distribution near the velocity of the bombarding ion. The α-particle production cross section measured in their work at forward angles was found to be considerably greater than the proton production cross section, whereas at backward angles the ratio of the proton and α-particle cross sections corresponded to the value calculated in the evaporation model. The authors interpreted this interesting result as due to breakup of the α-cluster bombarding nucleus in the field of the target nucleus. However, subsequent experiments made with heavier ions ($A_p \geqslant 20$), whose structure

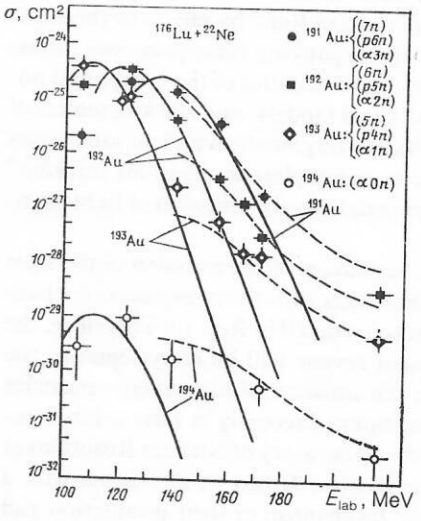

FIG. 1. Excitation functions for different entrance channels of the ^{176}Lu + ^{22}Ne reaction. The continuous curves are calculated in accordance with the statistical model.

 0090-4759/86/020065-28$04.40

TABLE I. Ratio of cross sections σ_α for production of α particles to the total cross section σ_R for different reactions.

Reaction	Ion energy, MeV	σ_α/σ_R	Reference	Reaction	Ion energy, MeV	σ_α/σ_R	Reference
$^{12}C+^{209}Bi$	126	0,60	[1]	$^{22}Ne+^{232}Th$	140	0,41	[11]
$^{12}C+^{209}Bi$	105	0,37	[1]	$^{40}Ar+^{116}Sn$	274	0,49	[12]
$^{12}C+^{197}Au$	126	0,63	[1]	$^{40}Ar+^{197}Au$	274	0,36	[12]
$^{14}N+^{197}Au$	147	0,46	[1]	$^{40}Ar+^{197}Au$	340	0,44	[12]
$^{16}O+^{197}Au$	168	0,47	[1]	$^{22}Ar+^{181}Ta$	178	0,44	[3]
$^{16}O+^{209}Bi$	168	0,44	[1]				

differs appreciably from the α-particle configuration of nuclei of the ^{12}C or ^{16}O type, showed that the cross section for the production of high-energy particles can constitute an appreciable fraction of the total reaction cross section. Moreover, as was shown in Refs. 2 and 3, the large integrated cross section for the production of α particles in heavy-ion reactions does not prevent the emission with high probability of other more complicated charged particles and protons.

Here and in what follows, by high-energy particles we shall understand particles whose yield appreciably exceeds the calculated value at the corresponding energy in the evaporation model. Heavy-ion reactions are usually classified in accordance with the impact parameter or the entrance angular momentum. From zero angular momentum up to some critical angular momentum $l = l_{cr}$, the main reaction channel is the production of a compound nucleus as a result of complete fusion of the colliding nuclei.[1)] At the largest angular momenta $l \sim l_{gr}$ corresponding to grazing collisions, for which the nuclear forces only begin to be manifested, direct processes take place. Finally, at impact parameters corresponding to the range of angular momenta between l_{cr} and l_{gr} various deep inelastic processes take place.[4–6] It is natural to attempt to relate reactions with the emission of fast particles to one of these basic reaction channels and use this connection to interpret some of the features of these reactions. Thus, the energy shedding in deep inelastic transfer reactions and also the angular momentum of the products of these reactions are explained in Ref.7 by means of the emission of light particles accompanying these processes. Some deviations of the decay characteristics of the compound nuclei from ordinary statistical models[8] and the kinematics of the emission of their fission fragments, which is some cases appear to correspond to incomplete momentum transfer,[9] are also interpreted using data on the emission of light particles.

The question of the sources of the emission of the light particles and their connection with the main reaction channels was considered in some detail in Ref. 10. Therefore, the main task of the present review will be to systematize the experimental data on the emission of high-energy particles in heavy-ion reactions obtained recently in various laboratories, in the first place the Laboratory of Nuclear Reactions at the Joint Institute for Nuclear Research at Dubna, with a view to elucidating the mechanism of their production and also the possibilities of using these processes to obtain nuclei with unusual properties and to investigate them.

1. CROSS SECTIONS FOR THE PRODUCTION OF LIGHT CHARGED PARTICLES IN HEAVY-ION REACTIONS

In reactions with heavy ions with mass up to $A_p \leqslant 40$ and energy up to 10 MeV/nucleon, α particles are produced with a large cross section. Table I gives the α-particle production cross section relative to the total reaction cross section σ_R for various target–bombarding-ion combinations.

The total reaction cross section was calculated in accordance with the expression $\sigma_R = \pi R^2(1 - V_{Co}/E_{cms})$, where $R = r_0(A_t^{1/3} + A_p^{1/3}) + 0.5$ F (A_t and A_p are the masses of the target and the ion, and V_{Co} is the Coulomb barrier). It can be seen that the α-particle production cross section reaches, and in some cases even exceeds, half the total reaction cross section. The yield of these particles depends on the energy of the incident ion and, as was shown in Ref. 13, increases exponentially with increasing energy of the bombarding ion.

In inclusive measurements, it is rather difficult to separate all the components in the particle spectrum; however, using the angular distributions, one can separate the evaporation component and assume that the remaining α particles are the product of direct processes.

As was shown in Refs. 14 and 134, the number of evaporation α particles increases linearly with increasing excitation energy. In that work, an investigation was made of the formation of a compound nucleus following a collision of ^{12}C ions with ^{182}W nuclei, the excitation energy being varied from 57 to 142 MeV, which was accompanied by an increase in the cross section of evaporation particles from 5 to 28% of the fusion cross section.

Figure 2 shows the dependence of the yield of direct α particles on the energy above the Coulomb barrier of the colliding nuclei, calculated for one nucleon. The resulting smooth curve indicates the existence of a threshold for the emission of such particles, above which the cross section for their production increases rapidly and then, above an energy of about 5 MeV/nucleon, remains at one level. A similar conclusion was also drawn in Ref. 16, in which it was noted that there must exist a certain relative velocity for realization of the emission of direct particles.

With a relatively high probability and above a certain threshold energy of the bombarding ion, other light charged particles—*d*, *t*, He, and the nuclei of the light elements Li and Be—are formed in direct processes.

Table II gives the cross sections of the isotopes of the

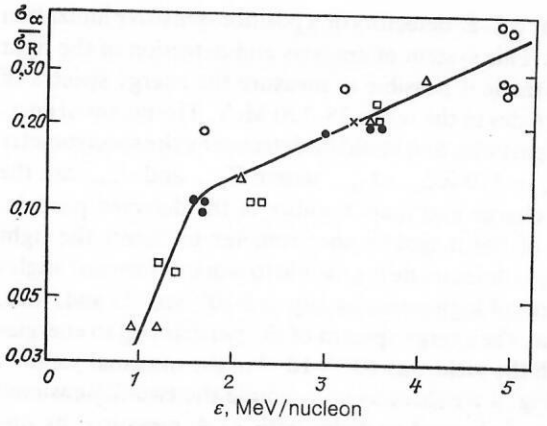

FIG. 2. Dependence of the yield of α particles on the energy ε above the Coulomb barrier of the colliding nuclei. Data from different studies are indicated by the following symbols: Open circles from Ref. 1, open squares from Ref. 12, the cross from Ref. 3, open triangles from Ref. 13, and black circles from Ref. 15.

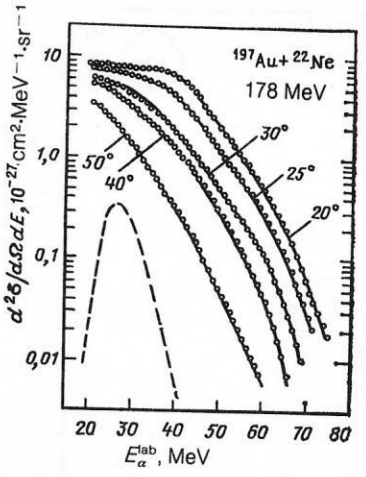

FIG. 3. Energy spectra of α particles measured at different angles for the $^{197}Au + {}^{22}Ne$ reaction. The continuous curves are drawn through the points, and the broken curve is a calculation in accordance with the statistical model.

elements from H to Be, measured in Ref. 17 for the $^{181}Ta + {}^{22}Ne$ reaction. In the same table we give the calculated cross sections obtained by means of the phenomenological "sum-rule" model of Ref. 18. This model is based on the assumption of mass transfer of a fragment of the projectile nucleus to the target nucleus. It can be seen from the table that there is good agreement for the production cross sections of some particles as measured experimentally and predicted by the model. In all probability, contributions of different processes may contribute to their production cross section. In all experiments with heavy ions, an enhanced contribution of α particles compared with other charged particles, including protons, was observed. There is no unambiguous explanation of this phenomenon, although in some studies the enhanced α-particle yield is explained by their low binding energy in other nuclei or by the existence of clustering. It was shown in Ref. 19 that compound nuclei with high angular momenta can emit complex particles with a probability much greater than that predicted by the classical evaporation model. Measurements made by a group at Stony Brook[20] showed that at ion energies around 10 MeV/nucleon and higher the heavy compound system, having no fission barrier, emits lighter particles with a greater probability than fissioning. In Ref. 21, it was shown that the cross section for the production of light particles in heavy-ion reactions can be described by the so-called Q_{gg} systematization, i.e., the cross section for the emission of different isotopes of a given element is proportional to $\exp(Q_{gg}/T)$ (Q_{gg} is the difference between the masses of the initial and final nuclei, and T is the temperature of the system).

Thus, further study of the cross sections for the production of light charged particles in reactions with heavy ions can help to give new information about the mechanism of this process.

2. ENERGY SPECTRA OF LIGHT CHARGED PARTICLES

Despite the variety of reaction channels with which the emission of light particles can be associated, important information about the mechanism of their production can be obtained from measurements of the inclusive energy spectra at different angles. The first experiments to measure the energy spectra of α particles, made using the U-300 cyclotron of the Laboratory of Nuclear Reactions at Dubna with a telescope of semiconducting ΔE–E detectors as a detecting system, revealed an appreciable difference between the experimental spectra and those calculated using an evaporation model.[22] Figure 3 shows the energy spectra of the α

TABLE II. Experimentally measured cross sections for the production of different isotopes in the $^{181}Ta + {}^{22}Ne$ reaction[17] and cross sections calculated in the sum-rule model.[18]

Cross section	p	d	t	^{3}He	α	^{6}He	^{8}He
σ_{exp}, 10^{-27} cm^2	12.2	16.8	11.0	0.65	460	1.1	0.002
σ_{cal}, 10^{-27} cm^2	22.5	3.6	3.02	0.57	270	0.8	0.0006

Cross section	^{6}Li	^{7}Li	^{8}Li	^{9}Li	^{9}Be	^{10}Be
σ_{exp}, 10^{-27} cm^2	1.3	3.5	0.55	0.066	9.0	6.5
σ_{cal}, 10^{-27} cm^2	2.3	5.2	0.22	0.47	9.8	5.5

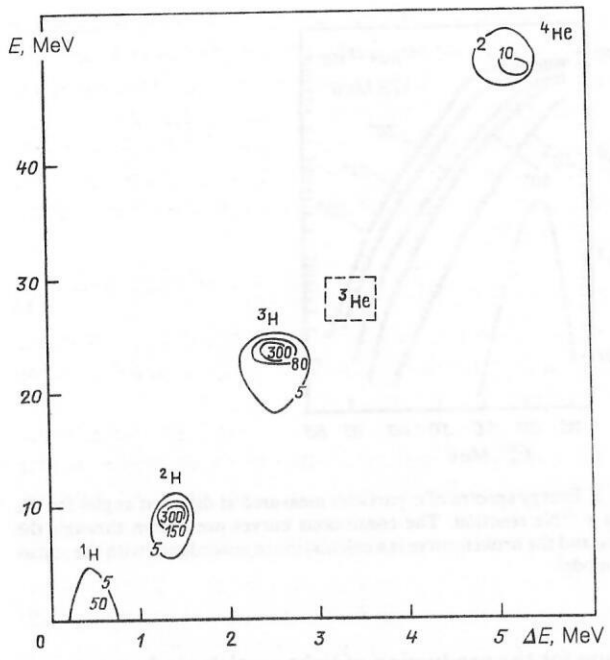

FIG. 4. The ΔE–E matrix taken for the $^{197}Au + ^{22}Ne$ (178 MeV) reaction at $\theta_{lab} = (0 \pm 2)°$. The telescope of semiconducting ΔE–E detectors was set up in the focal plane of the magnetic spectrometer.

particles for the $^{197}Au + ^{22}Ne$ reaction measured at different angles. In the same figure, we give for comparison the calculated spectrum of the evaporation α particles from the compound nucleus. It can be seen that the experimental and calculated spectra differ strongly. These data confirm the previously known fact of a significant increase of the yield of α particles in the region of small angles in heavy-ion reactions. In addition, it follows from these data that there is a relatively high probability for the production in the reaction of α particles with velocities exceeding by several times the velocity of the bombarding ions, the spectrum becoming significantly harder with decreasing detection angle. Thus, the most energetic α particles are emitted along the direction of the primary ion beam ($\theta = 0°$). In this connection, it was necessary to place the detector at the angle 0° in the experiments to measure the emission of high-energy particles.

Methodologically, such an experimental arrangement involves certain difficulties because of the heavy loading of the detectors by the nuclei of the bombarding beam. In order to separate the reaction products from the beam at forward angles, it was necessary to use a separating device in the experiments. In those made at Dubna, the magnetic spectrometer MSP-144 was used for this purpose. The spectrometer is a wide-range magnetic analyzer with stepped poles. The energy range of the reaction products that could be detected by the spectrometer was $E_{max}/E_{min} = 5.2$ with energy resolution $\Delta E/E = 5 \cdot 10^{-4}$. The spectrometer had good linearity of the focal plane over its complete length of 1500 mm, and also a linear dependence of the dispersion and resolution on the position in the focal plane. The solid angle of the spectrometer was 5 msr and the deflection angle of the particles was 110.7°. The particle detector employed was either a system of telescopes of semiconductor ΔE–E detectors or a position-sensitive ionization chamber. This system of analysis and detection of the light particles made it possible to measure the energy spectra of the α particles in the range 25–120 MeV. The maximal energy of the particles that could be detected by the spectrometer was $E_{max} = 120\, Z^2_{part}/A_{part}$, where Z_{part} and A_{part} are the effective charge and mass number of the detected particle. The use of the magnetic spectrometer to detect the light charged particles made it possible to work at forward angles with beams of high intensity (up to $5 \cdot 10^{13}$ sec^{-1}) and, thus, to measure the energy spectra of the particles up to energies for which the yield was 10^{-6}–10^{-8} of the maximal yield.

In Fig. 4 we show as an example the two-dimensional spectrum of charged particles with $A \leqslant 4$, measured by one telescope of semiconductor ΔE–E detectors at a definite rigidity of the magnetic field. The employed system made it possible to separate and identify reliably the different light particles. We consider now the characteristic features of the energy spectra measured by means of the method described above.

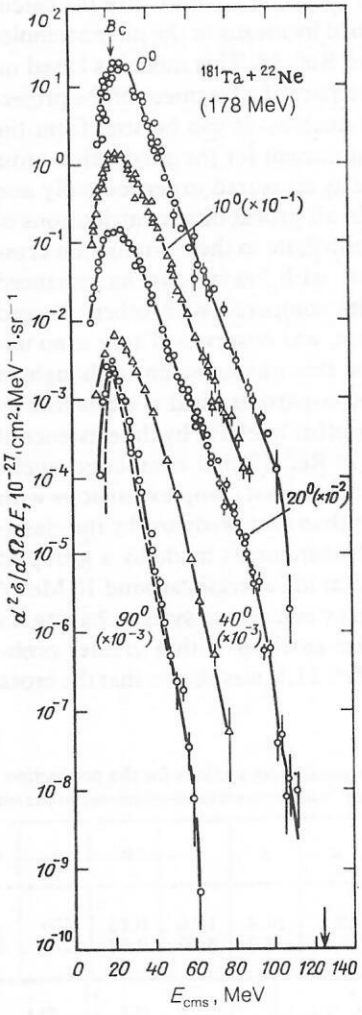

FIG. 5. Energy spectra of α particles measured at different angles and represented in the center-of-mass system. The continuous curves are drawn through the experimental points, and the broken curve represents the results of a calculation in accordance with the evaporation model for the angle 90°. The arrow at the top shows the energy corresponding to the exit Coulomb barrier.

Most probable energy of the particles

At energies of the bombarding ions lower than 10 MeV/nucleon, the Coulomb potential energy plays an important part in the interaction of two complex nuclei. It significantly reduces the kinetic energy of the bombarding nucleus in the entrance channel, and also changes the energy of an emitted particle. Practically all the energy spectra of light charged particles measured at backward angles ($\theta \geqslant 90°$) have a maximum coincident with the exit Coulomb barrier for the given particle. This result is interpreted in the framework of an evaporation model of the compound nucleus. At the same time, it must be borne in mind that for the considered bombarding energies particles evaporated from an excited product of the transfer reaction can also have a maximum of the distribution near the exit Coulomb barrier for the compound nucleus. This can be shown by considering the kinematics of the products in the laboratory coordinate system and adding the velocity of the particle to the velocity of the emitter nucleus.

The position of the maximum in the energy distributions of the light charged particles measured at forward angles is displaced in the direction of the energy corresponding to the velocity of the incident ion (Fig. 5). The most probable energy of the particles emitted in heavy-ion reactions can be estimated in the framework of the sum-rule model.[18] Using the assumption of this model—that the introduced angular momentum is distributed between the emitted particle and the residual nucleus in proportion to their masses—one can extend this assumption to the momentum transfer.[17] Then the particles emitted at angle θ with mass number A_x carry away momentum $P_x = P_p \cos\theta (A_x/A_p)$, where P_p is the momentum of the incident particle after it has overcome the entrance Coulomb barrier $V_{Co}(R)$, A_p is the mass of the incident particle, and A_x is the mass of the emitted particle. If we take into account the binding energy E_s of the particle in the incident ion, and also the dissipation energy E_D, which is an adjustable parameter of the model and takes into account the possibility of heating of the target nucleus, we can obtain an expression for the most probable energy of the emitted particle:

$$E_x = E_{Co}(R) + (E_p - V_{Co}(R) - E_s - E_D)\frac{A_x}{A_p}\cos^2\theta - E_R, \quad (1)$$

where $E_{Co}(R)$ is the exit Coulomb energy of the particle, E_p is the c.m.s. energy of the incident particle, and E_R is the recoil energy.

The most probable energies of the emitted particle calculated in this manner agree with the experimental values for different particles irrespective of the angle of observation.[17] It follows from Eq. (1) that at high energies of the incident ion the maximum of the energy distribution will approach the energy corresponding to the velocity of the incident ion, while at small E_p the most probable energy will be basically determined by the Coulomb term $E_{Co}(R)$. It should here be noted that the sum-rule model also predicts with good accuracy the cross section for the production of light particles in reactions with accelerated heavy ions with $A_p \leqslant 20$.[17,23]

Slopes of the energy spectra

All the energy spectra of the light charged particles fall off exponentially at high energies. The slope of the exponential curve depends strongly on the energetics of the reaction and on its mechanism.[24] Therefore, from the slopes of the

TABLE III. Characteristics of the energy spectra of different isotopes formed in reactions with ^{22}Ne heavy ions on different targets; $E_{max.part}$ is the energy at the maximum of the spectrum, V_{Co} is the exit Coulomb barrier, FWHM and T_{eff} are the half-width of the energy spectrum and the effective temperature, $d\sigma/d\Omega$ is the differential cross section for production of the isotope, and E^{cal}_{max} is the calculated kinematic limit (all quantities are given in the center-of-mass system).

Particle	^{181}Ta + ^{22}Ne (E_p=178 MeV)						^{232}Th + ^{22}Ne (E_p = 178 MeV)					
	$E_{max.part}$, MeV	V_{Co}, MeV	FWHM, MeV	T_{eff}, MeV	$\frac{d\sigma}{d\Omega}$, 10^{-27}cm^2/sr	E^{cal}_{max}, MeV	$E_{max.part}$, MeV	V_{Co}, MeV	FWHM, MeV	T_{eff}, MeV	$\frac{d\sigma}{d\Omega}$, 10^{-27}cm^2/sr	E^{cal}_{max}, MeV
p	10	11,5	7	4,0	238	120,3	11	13	7	4,8	705	103,3
d	12,5	11,0	8	4,9	33	113,3	16	12,5	18	7.7	138	98,3
t	13.5	10.8	10,5	5,4	21	112,1	21	12,3	25	—	110	99,4
^{3}He	29.5	21.3	16	4.7	1,2	112,7	—	24,3	19	4,5	4,8	99.8
^{4}He	25	21,0	13	5,6	725	125,2	26,5	23,9	18	7,1	2050	114.6
^{6}He	28.5	20,4	14	7,1	1.7	110,9	35	23,2	29	12,8	2.8	102,7
^{8}He	—	19,9	—	—	—	94,6	29,5	22,8	6	3,3	0.0043	91.3
^{6}Li	—	30,2	—	5,7	—	115.4	49	34,4	14	5.9	7.9	105,0
^{7}Li	—	29,8	—	5,8	—	115,1	47	34,1	17	8,1	11.1	106.6
^{8}Li	—	29,5	—	5.1	—	107.9	48	33,8	20	10,7	0.7	101.7
^{9}Be	—	38,6	—	7,0	—	117,6	—	44,2	—	5,1	—	113.5
^{10}Be	—	—	—	—	—	—	—	43,9	—	5,5	—	114.3

Particle	Ti + ^{22}Ne (E_p = 178 MeV)						Ti + ^{22}Ne (E_p = 196 MeV)					
	$E_{max.part}$, MeV	V_{Co}, MeV	FWHM, MeV	T_{eff}, MeV	$\frac{d\sigma}{d\Omega}$, 10^{-27}cm^2/sr	E^{cal}_{max}, MeV	$E_{max.part}$, MeV	V_{Co}, MeV	FWHM, MeV	T_{eff}, MeV	$\frac{d\sigma}{d\Omega}$, 10^{-27} cm^2/sr	E^{cal}_{max}, MeV
^{3}He	—	10,5	—	4.3	—	113.4	16,5	10,5	15	4,3	4.4	127,9
^{4}He	13	10,2	13	4.8	738	124,5	14	10.3	14	5,2	510	137,8
^{6}He	17,5	9,9	16	5.9	1,2	104.2	20	10,0	18	5,1	0,3	115,2
^{8}He	16,5	9.7	7,5	3,5	0,0062	84,2	—	9,7	—	2.5	—	93,0
^{6}Li	20	14,4	—	4,0	—	106.9	24.5	14,5	15	4,2	3,5	119.9
^{7}Li	24,5	14,2	—	4,5	—	104,6	25	14.3	16	4,8	2,6	116,5
^{8}Li	25	14.0	—	5,0	—	95.1	25	14,1	18	4,8	0.17	106.1
^{9}Be	31	17.9	—	3,0	—	103.2	—	18.0	—	4.0	—	115.1
^{10}Be	31	17,7	—	4,3	—	100,6	36	17,8	—	4.1	—	111,2

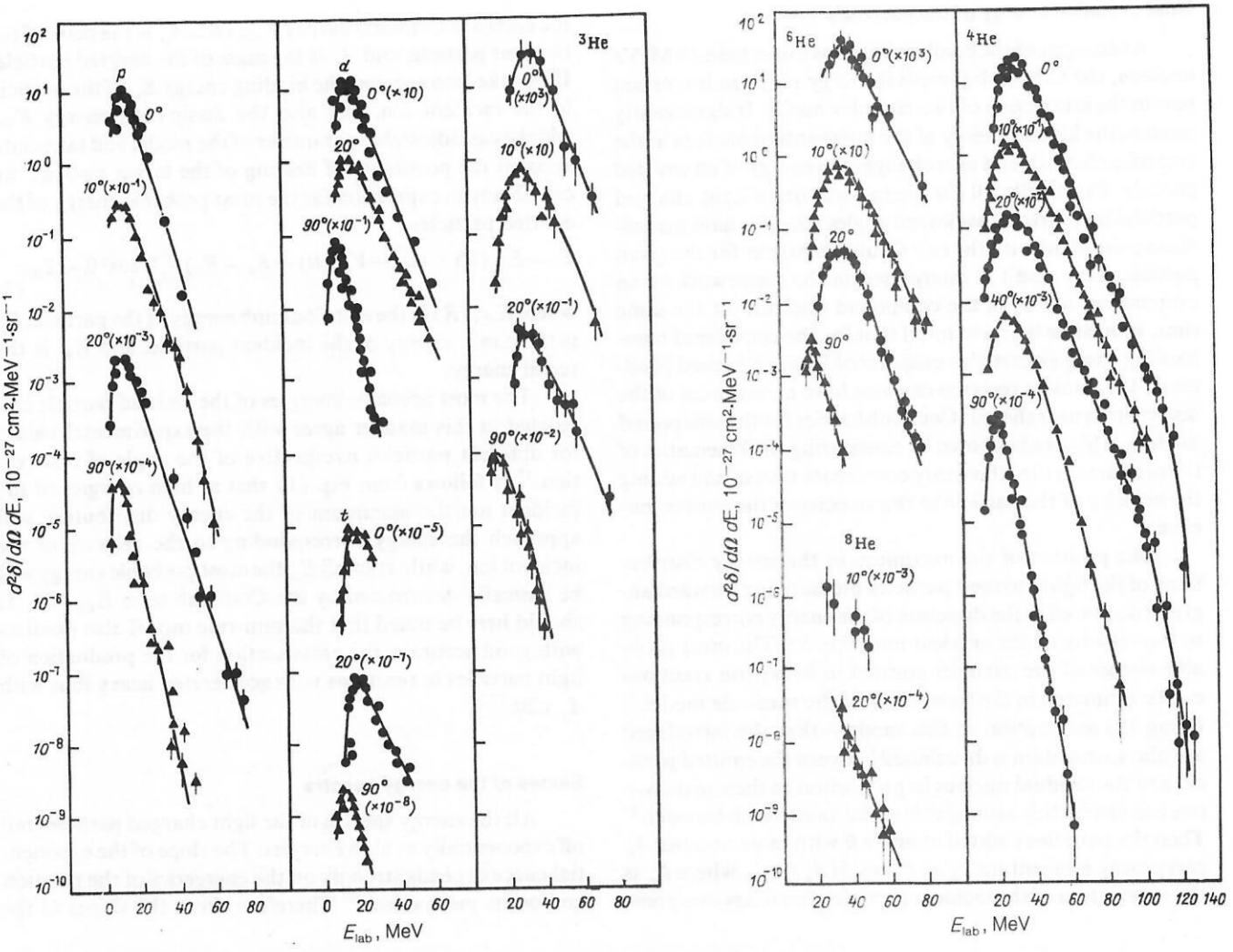

FIG. 6A. [*Translation Editor's Note.* This figure appeared without a caption in the Russian edition.]

spectra it is possible to extract important information about the interaction of two complex nuclei.

In the case of particle evaporation from a compound nucleus, for which a uniform energy distribution between the nucleons can be assumed, a thermodynamic approach is usually employed to describe the spectra. In accordance with this approach, the energy distribution of the emitted particles can be expressed in the form

$$N_x = N_0 E_x \sigma_c (E_x) \exp(-E_x/T), \qquad (2)$$

where N_0 is a constant coefficient, E_x is the energy of the emitted particle, and $\sigma_c(E_x)$ is the absorption cross section of the particle.

In reactions with heavy ions, the energy spectra of light particles (n, p, α) observed at backward angles or at low bombarding energies can be well described by the expression (2). In this case, the parameter T is intimately related to the excitation energy (E^*) of the compound nucleus by the relation $T = (E^*/a)^{1/2}$, where a is the level-density parameter. Without interpreting the parameter T as a temperature and regarding it as an adjustable parameter that characterizes the slope of the energy spectrum, it is possible to find its value for any spectrum, using Eq. (2). Table III gives the values of the parameter T obtained in Ref. 2 for different reactions accompanied by the emission of different particles. As can be seen from the table, the effective temperature increases for a given element with increasing mass of the target and mass of the emitted particle (the ^{8}He nucleus is an exception).

The energy spectrum of the light particles becomes harder with decreasing angle of their emission. Figure 6 shows the energy spectra of nuclei with $Z = 1$–4, measured in Ref. 3 by means of a magnetic spectrograph at different angles. Comparison of the experimental energy spectrum of the light particles with those calculated in accordance with the evaporation model shows that in all the spectra measured at forward angles an appreciable contribution of the pre-equilibrium component is observed, irrespective of the energy of the bombarding ions up to angles 90°. As was shown in Ref. 3, at angles greater than 40° particles with $Z > 3$ were not observed at the sensitivity level of the experiment [10^{-33} cm^2·MeV^{-1}·sr^{-1}]. This indicates that these nuclei are produced in the reaction only in the direct process.

In Ref. 25, a smooth dependence of the parameter T on

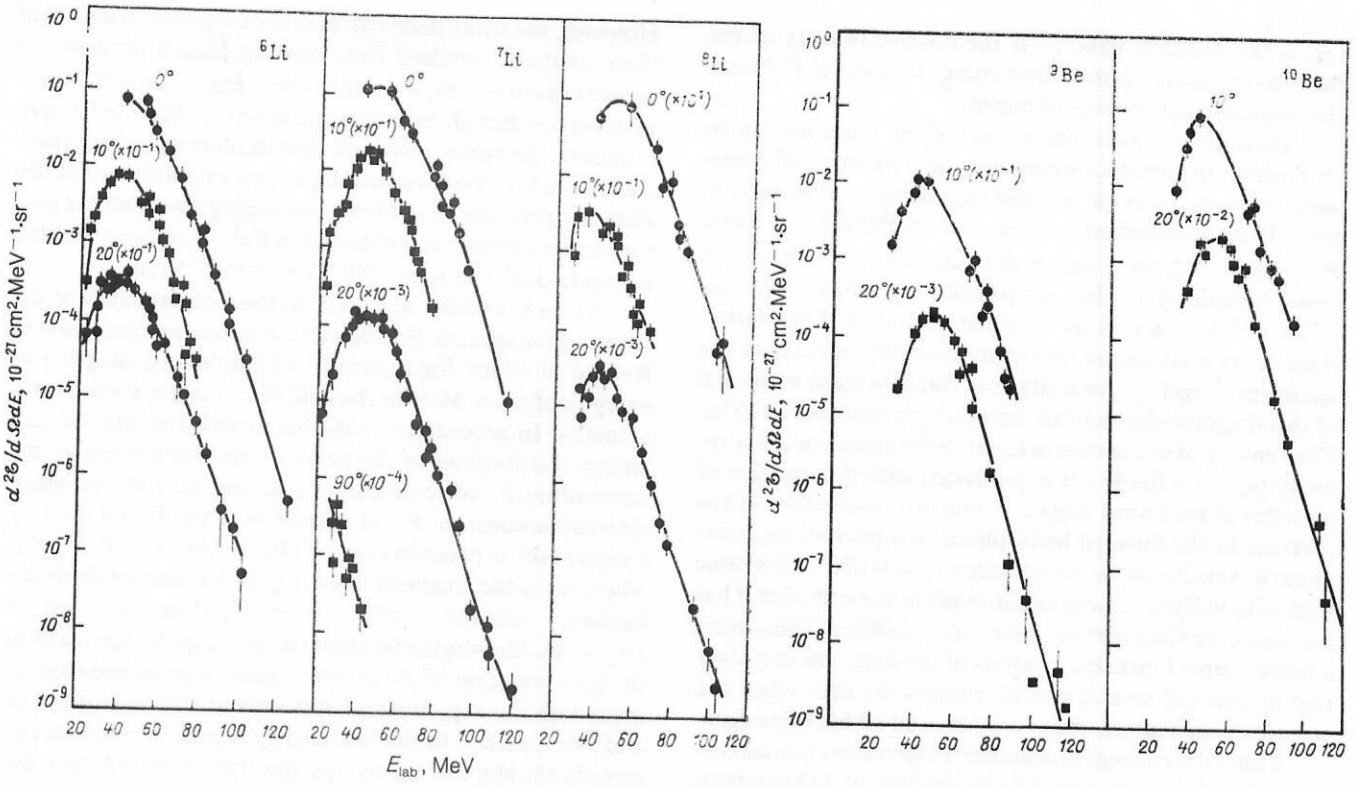

FIG. 6B. Energy spectra of lithium and beryllium isotopes measured in the ^{181}Ta + ^{22}Ne (E_p = 178 MeV) reaction at different angles. The curves are drawn through the experimental points.

the angle was obtained in the description of the energy spectra of α particles produced in reactions with ^{14}N ions at different angles. At forward angles, the so-called experimental "temperature" greatly exceeded the equilibrium temperature. It was only at angles greater than 170° that the two values were equal. It was concluded that such behavior of the temperature can be explained by assuming the existence of an evolution of the excitation energy from the initial phase, when there is a small number of excited nucleons localized on the surface of the nucleus, to the final stage, when the excitation extends to a large number of nucleons, this leading to a decrease in the temperature. Such an explanation of the reaction mechanism was proposed by Weiner and Weström,[26] who introduced for the first time the concept of a "hot spot." This approach was subsequently intensively developed in Ref. 27–29.

Transforming Eq. (2) for a moving system, Awes *et al.*[30–32] achieved a satisfactory agreement between the calculated and experimental p, d, t, and α spectra obtained for the interaction of accelerated ^{16}O ions (310 MeV) with heavy nuclei. In Ref. 32, the temperature T was observed to increase linearly with increasing projectile velocity. This fact was explained in the framework of the Fermi-gas model. Writing the temperature in this case as

$$T = (2m_0 v_p^2 \varepsilon_F/\pi^2)^{1/2} \tag{3}$$

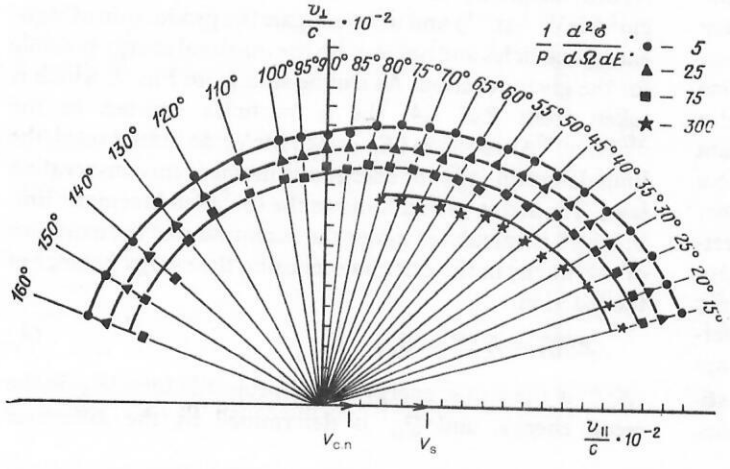

FIG. 7. Diagram of Lorentz-invariant cross section for α particles from the ^{181}Ta + ^{22}Ne reaction. The curves are drawn through points with the same values of $(1/P)(d^2\sigma/d\Omega\, dE)$. The arrows indicate the velocities of the compound nucleus and the velocity of the source that contributes to the emission of α particles at forward angles; $v_\parallel$ and $v_\perp$ are the longitudinal and transverse components of the α-particle velocity.

(m_0 is the nucleon mass, v_p is the relative velocity of the incident ion, and ε_F is the Fermi energy), values of T close to the measured values were obtained.

Information about the source of the particles can be obtained from the velocity diagram, the experimentally measured cross sections $(d^2\sigma/dEd\Omega)_{lab}$ being transformed to the Lorentz-invariant form $(d^2\sigma/PdEd\Omega)$, where $P=\sqrt{2mE}$. Figure 7 shows the diagram of the invariant cross section for the α particles produced in the $^{181}Ta + {}^{22}Ne$ reaction as obtained in Ref. 3. For clarity, these cross sections are shown in their dependence on the velocities $v_{\parallel}$ and $v_{\perp}$. An analysis of the data made by means of this diagram showed that two particle sources can exist. The velocity of one source is equal to the center-of-mass velocity ($v_{c.n} = 0.0143c$); it is associated with the emission of particles at backward angles. From the distribution of the particles in the forward hemisphere, it is possible to determine the velocity of the other source: $v_s = 0.053c$. This value is close to half the velocity of the incident particle after it has overcome the Coulomb repulsion ($v_0 \sim 0.089c$). Thus, using a fairly simple kinematic analysis of the data, one can show that in principle several particle sources can exist when two complex nuclei interact at energy around 10 MeV/nucleon.

Using the concept of a source temperature, one can obtain other characteristics of the process of light-particle emission. For example, using the dependence of the parameter T on the particle emission angle, we can estimate the time of rotation of the system until emission of a particle. In Ref. 3, in which it was assumed that there is a change in the temperature as a function of the time[33] in accordance with $\Delta T = \Delta T_i \exp(\Delta t/\tau)$ (Δt is the interval of time and τ is a constant), an estimate was made of the velocity of the hot spot in the case of bombardment by ^{22}Ne ions (178 MeV) of ^{181}Ta nuclei, which for this case was found to be about 10^{-21} rad/sec, and of the mean value of the rotation angle of the system, which was 40°. Using the assumption of a peripheral collision and a rigid-body moment of inertia, the lifetime of the hot spot was found to be $7\cdot10^{-22}$ sec.

At the same time, all arguments relating to the interpretation of the slope of the energy spectrum and its relation to the temperature of such a source become meaningless if the spectrum has several components with nearly equal intensities. Such a possibility was demonstrated by the measurement of the spectrum of α particles with simultaneous separation of the channel of the xn reaction by coincidence with γ photons in the $^{116}Sn(^{16}O, \alpha xn)$ reaction (125 MeV). The α-particle spectrum was observed to have two maxima—one with an energy close to the exit Coulomb barrier for the α particle, the other at an energy corresponding to the beam velocity, the intensities of these components depending to a large degree on the reaction channel.[15] There are a number of other factors which indicate a possible error in interpreting the slope of the spectrum as the temperature of the nucleus. In Ref. 34, measurements were made of the energy spectra of neutrons in coincidence with nuclei as transfer-reaction products. The inclusive neutron spectra differed appreciably from those calculated in accordance with a statistical model of evaporation from a compound nucleus. However, the study demonstrated the evaporation nature of these neutrons, emitted from moving heated products of transfer reactions. Separating in the energy spectra the components associated, respectively, with the light and heavy products, the authors showed that the corresponding spectra have in their rest systems slopes agreeing with an equilibrium temperature (2–3 MeV). An analogous result for protons and α particles was obtained in Ref. 35 in the case of the interaction of ^{40}Ar ions (280 MeV) with ^{58}Ni nuclei.

There is another approach to the interpretation of the slopes of the spectra. For example, a model was proposed in Ref. 36 in which fragmentation of the bombarding ion at energies of a few MeV in the field of the target nucleus was assumed. In accordance with this model, the angular and energy distributions of the particles are determined by the momentum P_p of the incident ion, and also by the mean internal momentum P_F of a nucleon at the Fermi level by means of the expression $\exp[-(P_F - (m_f/m_p)P_p)^2/\sigma^2]$, where m_f is the fragment mass, m_p is the mass of the bombarding nucleus, and $\sigma^2 = (P_F^2/5)m_f(m_p - m_f)/(m_p - 1)$. Despite the fact that such an impulse approach to the interpretation of the inclusive spectra gives good agreement with the experimental data only at high energies, Lee and Wu[37] used it in the low-energy region. In such an approach, the slope of the energy spectrum does not have the meaning of a temperature but merely determines the accessible phase space. However, in Ref. 38 an attempt was made formally to relate σ to a temperature, and this yielded the dependence $\sigma_0^2 = mT(A-1)/A$, where m is the nucleon mass and A the mass of the system.

Maximal energy of light particles

The exponential decrease of the energy spectrum described by the expression (2) must extend to a limit determined by the reaction energetics. The investigation of the energy spectra of light charged particles near the limiting energies at limiting angles is a complicated methodological problem because of the need to separate a process that takes place with a cross section $\leqslant 10^{-34}$ cm^2 on the background of reaction products produced with a cross section 6–7 orders of magnitude greater. The use of a magnetic spectrometer and intense heavy-ion beams (up to $1.5\cdot10^{13}$ sec^{-1}) made it possible for the authors of Refs. 2, 3, and 24 to achieve a record sensitivity for such experiments (of order 10^{-33} cm$^2\cdot$MeV$^{-1}\cdot$sr^{-1}) and to investigate the production of high-energy particles and nuclei with the maximal energy possible for the given reaction. As can be seen from Fig. 7, which is taken from Ref. 24, the α particles emitted in the $^{232}Th + {}^{40}Ar$ reaction ($E_p = 220$ MeV) do indeed reach the limit determined by the energy and momentum conservation laws. The arrow in Fig. 8 shows the so-called kinematic limit, which is calculated under the assumption of the existence of two nuclei in the exit channel using the energy balance of the reaction:

$$E_{max}^{cms} = E_p^{cms} - Q_{gg} - E_R \qquad (4)$$

(E_p^{cms} is the c.m.s. energy of the projectile ions, E_R is the recoil energy, and Q_{gg} is determined by the difference

TABLE IV. Calculated values of Q_{gg} of the reaction, the Coulomb repulsion energy $V_{Co,2-3}$ of the nuclei, and the maximal energy of the α particles in the c.m.s., $E^{cms}_{\alpha max}$, and laboratory system, $E^{lab}_{\alpha max}$, for different exit channels of the reaction.

Reaction	(1)	(2)	(3)	(4)	(5)	(6)
Q_{gg}	−31.0	−9.7	1.5	94.7	111.0	—
$V_{Co,2-3}$	—	70.5	84.3	168.8	179.5	—
$E^{cms}_{\alpha max}$	125.2	76.9	74.4	82.9	88.4	—
$E^{lab}_{\alpha max}$	139.3	88.1	85.4	94.5	100.4	~60

between the masses of the initial and final products). It follows from the experimental data obtained on the maximal energies of α particles in heavy-ion reactions[24] that this energy is only a few MeV below the maximal possible energy (E_{max}) that the ^{4}He nucleus can carry away. Such a situation can arise only when the incident ion transfers almost the entire momentum to the emitted particle, the remaining mass being absorbed by the target nucleus. A calculation shows that the formation of any third product in the exit channel of the reaction leads to a significant decrease of the maximal energy of the emitted particle possible for the given reaction. Table IV gives the results of calculations of the maximal possible energy of α particles produced in different channels of the ^{181}Ta + ^{22}Ne reaction[2]: in the two-body process with the ^{4}He and ^{199}Tl nuclei in the exit channel (1), for disintegration of the ^{22}Ne projectile into an α particle and an ^{18}O nucleus (2), knockout of an α particle from the target nucleus (3), symmetric and asymmetric fissioning of the ^{203}Bi compound nucleus with simultaneous emission of an α particle (4 and 5), and emission of an α particle from one of the fission fragments of the compound nucleus (6). It can be seen from the table that in the three-body processes the maximal energy of the third particle is appreciably reduced, despite the fact that Q_{gg} in many cases is smaller because of the energy of the Coulomb repulsion of the nuclei (V^{Co}_{2-3}). Thus, the formation of α particles with energy $E_\alpha > 100$ MeV in the ^{181}Ta + ^{22}Ne reaction is possible only in a two-body process. The same conclusion also follows for the emission of other high-energy charged particles. The values of the maximal possible energy calculated under the assumption of a two-body process (Figs. 8 and 9) agree well with the limiting values of the energy spectra for many of the investigated reactions. Correlation experiments, the results of which are given below, confirm this important conclusion.

The cross section for the emission of α particles with the limiting energy depends strongly on the combination of the colliding nuclei. Figure 8 shows the spectra of α particles produced by the bombardment of a thorium target by the ^{22}Ne and ^{40}Ar ions. Despite the fact that the cross section for the emission of α particles in the case of ^{40}Ar ions is lower than in the reaction with ^{22}Ne ions, the cross section at which the kinematic limit (E^{max}_α) is attained is several times higher in the case of ^{40}Ar. This fact may have a decisive

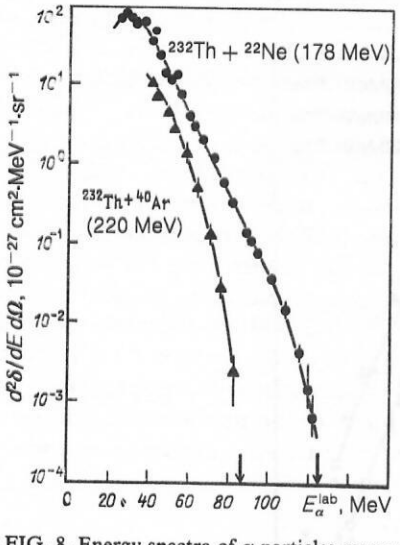

FIG. 8. Energy spectra of α particles measured at 0° from the reactions ^{232}Th + ^{40}Ar (220 MeV) and ^{232}Th + ^{22}Ne (178 MeV). The arrows indicate the greatest possible energies of the α particles calculated for two-body kinematics.

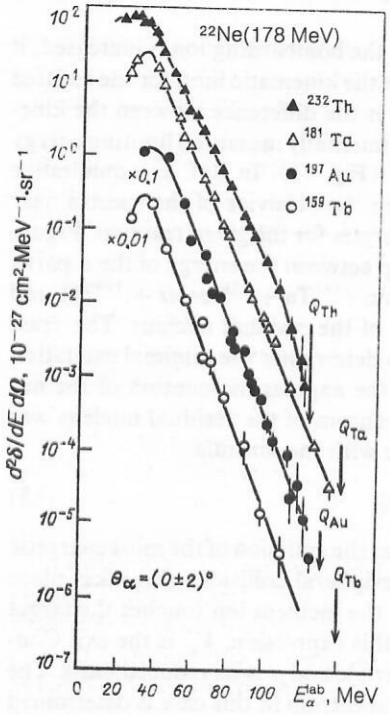

FIG. 9. The same as in Fig. 8 for reactions with ^{22}Ne (178 MeV) ions on different targets.

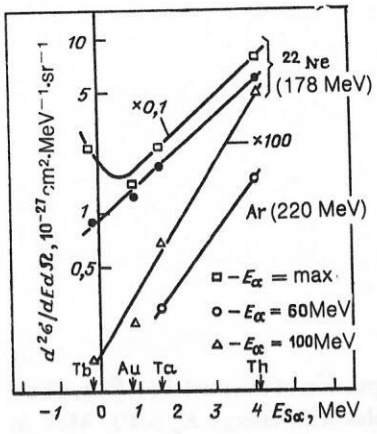

FIG. 10. Differential cross section for α particles of different energies as a function of the binding energy of an α particle in the target nucleus for reactions with the ions ^{22}Ne and ^{40}Ar.

significance when such processes are used to obtain heavy nuclei in the ground state (see Sec. 7). Analysis of the absolute cross sections for the production of α particles obtained in reactions with different targets made it possible to find a correlation between the cross section for the emission of α particles with energy $E_\alpha \geqslant 60$ MeV and the binding energy of α particles in the target nucleus.[24] Such a dependence is shown in Fig. 10, in which the abscissa is the energy release associated with emission of an α particle by the target nuclei ^{159}Tb, ^{181}Ta, ^{197}Au, ^{232}Th and the ordinate is a cross section for the emission of α particles with energy corresponding to 60, 100 MeV, and the maximum of the energy spectrum. The yield of α particles increases with increasing energy release when the α particle is stripped from the target nucleus. This correlation is most clearly revealed for the more highly energetic α particles.

When the energy of the bombarding ion is increased, it follows from Eq. (4) that the kinematic limit for the emitted particles is increased, as is the difference between the kinematic limit and the experimentally measured limiting energy in the particle spectrum (Fig. 11). In Ref. 2, a qualitative explanation was given for the behavior of the spectra near the maximal possible energies for the given reaction. Figure 12 shows the relationship between the energy of the α particle emitted in the reaction (^{181}Ta + ^{22}Ne→α + ^{199}Tl) and the angular momentum of the residual nucleus. The yrast line for the ^{199}Tl nucleus determines the minimal excitation energy as a function of the angular momentum of the nucleus. The angular momentum of the residual nucleus was calculated in accordance with the formula

$$l_\alpha^2 = R\,[\mu\,(E_\alpha - V_\alpha)] \qquad (5)$$

under the assumption that the emission of the most energetic α particles occurs for peripheral collisions and takes place from the point at which the incident ion touches the target nucleus at radius R. In this expression, V_α is the exit Coulomb barrier of the α particle and μ is its reduced mass. The limiting energy of the α spectrum in this case is determined by the point of intersection of the curve determined by Eq. (5) and the yrast line. Such a representation of the mechanism of emission of the high-energy particles gave good agreement with the experimental data. Thus, for the ^{181}Ta + ^{22}Ne reaction at ion energy 178 MeV the calculated kinematic limit is 125 MeV and the experimentally measured limiting energy of the spectrum is 115 MeV, in agreement with the calculated value (Fig. 12). In Ref. 39, calculations were made using a direct-interaction model, and these confirmed the interpretation considered above of the behavior of the spectra in the high-energy part. At the same time, a different explanation of the behavior of the energy spectra is possible; it is based directly on the direct measurements of the angular momenta of the nuclei produced after the emission of the high-energy particles and is considered below.

3. ANGULAR DISTRIBUTIONS OF LIGHT CHARGED PARTICLES

Figure 13 shows the angular distribution of α particles observed in collisions of ^{22}Ne ions (178 MeV) with ^{181}Ta nuclei. The shape of this distribution is characteristic for the angular distributions of light reaction products of heavy-ion reactions. The curve has a sharp rise in the region of small angles and a smoother shape at large angles, beginning at 90°. As was shown in Ref. 15, the shape of the angular distributions does not depend on the combination of the colliding nuclei. The angular distributions of the α particles measured in Ref. 15 for two reactions (^{146}Sm + ^{16}O and ^{154}Sm + ^{16}O) at the same energy of the ^{16}O ions were found to be the same. However, the angular distributions of the light charged particles depend strongly on the energy of the bombarding ions. This can be seen in Fig. 14, which shows the angular distributions of the α particles for two values of the velocities of the ^{16}O, ^{19}F, and ^{20}Ne ions. At low velocities of the bombarding ions, when they correspond to an energy near the Coulomb barrier, the angular distributions of the light charged particles become symmetric about 90°. This was convincingly demonstrated in Ref. 40, in which a study was made of the angular distributions of the α particles in the ^{77}Se + ^{40}Ar reaction and their symmetric shape was explained by the

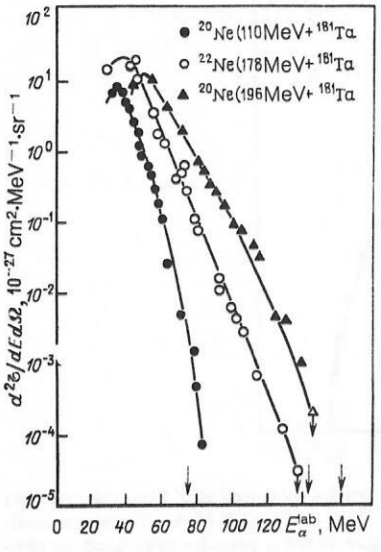

FIG. 11. The same as in Fig. 8, for the indicated reactions.

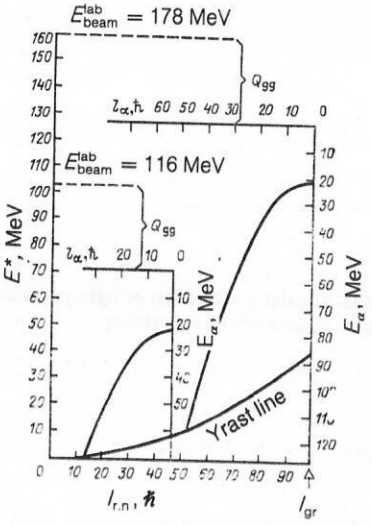

FIG. 12. Angular momentum of the residual nucleus as a function of the energy of the emitted α particle in the $^{181}Ta + {}^{22}Ne$ reaction for two neon energies: 116 and 178 MeV; E^* is the excitation energy of the residual nucleus, and l_α is the angular momentum carried away by the α particle.

absence in the energy spectra of the α particles of a high-energy component. Figure 15 shows the differential angular distributions of the α particles and protons obtained in Ref. 3. It can be seen that the angular distributions in different sections of the energy spectra behave differently—for the high-energy α particles and protons their angular distributions have a strong forward directionality, whereas the soft part of the spectrum changes little with the angle. Thus, the angular distributions of the light particles in the heavy-ion reactions give information about the components of the spectrum of these particles. In Ref. 41, an analytic expression was proposed for describing not only the asymmetric part of the angular distributions, $W_{as}(\theta) = A \exp(-b\theta - c\theta^2)$, but also the symmetric part, $W_{sym} = B + C\cos^2\theta$. A more complicated expression for the angular distribution of the light charged particles was obtained in Ref. 42: $W(\theta_{cms}) = W_0 \exp[(\beta_2/2)\sin^2\theta_{cm}] \times I_0[(\beta_2/2)\sin^2\theta_{cms}]$. In these expressions, A, B, C, W_0, and β_2 are parameters for fitting to the experiment, and I_0 is the Bessel function of zeroth order. As was shown in Ref. 43,

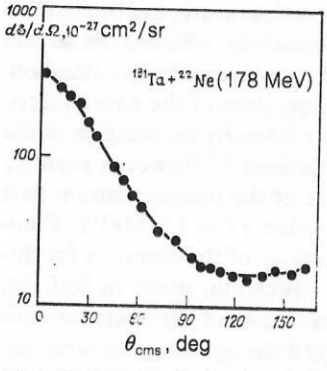

FIG. 13. Angular distribution of α particles from the $^{181}Ta + {}^{22}Ne$ (178 MeV) reaction.

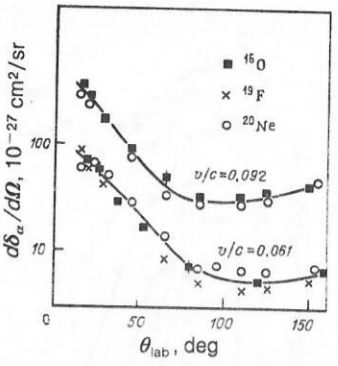

FIG. 14. Angular distributions of α particles for two velocities of the ions ^{16}O, ^{19}F, ^{20}Ne (from Ref. 15).

the parameter β_2 obtained in this manner makes it possible to determine the angular momentum of the residual nucleus.

Of great interest is information about the intensities of the pre-equilibrium and equilibrium components of the energy spectrum of the light particles as functions of the various reaction characteristics, including the velocity v/c of the incident ions. Figure 7 shows the dependence of these two components on v/c. As can be seen from the figure, the contribution of the pre-equilibrium component begins only above a certain threshold value of v/c.

Combined analysis of the angular and energy distributions of the light particles by means of variables invariant with respect to Lorentz transformation also makes it possible, as already noted in Sec. 2, to separate the components of the spectra of the particles and determine their sources. The method of invariant transformation of the cross sections is particularly convenient for interpreting correlation measurements, as well be shown in Sec. 6.

4. EMISSION OF HIGH-ENERGY NEUTRONS IN HEAVY-ION REACTIONS

From the point of view of the interpretation of the mechanism of emission of high-energy particles, the investigation of the emission of neutrons when heavy ions interact with nuclei is of great interest. Neutrally charged particles, which are not subject to the influence of the Coulomb fields, are, as it were, "indicators" of the temperature of the nuclei which emit them, and this is particularly important when one is considering theoretical models describing the process of emission of high-energy particles based on the assumption of a source of these particles in the region of interaction of the two nuclei.

Unfortunately, experimental data on the emission of high-energy neutrons in heavy-ion reactions are sparse, this being due to the methodological difficulties of performing such experiments, which are based mainly on the time-of-flight technique.

One of the first studies that revealed a component in the neutron energy spectrum corresponding to high-energy neutrons was that of Sarantites *et al.*,[44] who measured the neutron spectra for the interaction of the relatively light ^{12}C ions with the ^{158}Gd target. It should be noted that experimental investigations of neutron spectra made at about the same

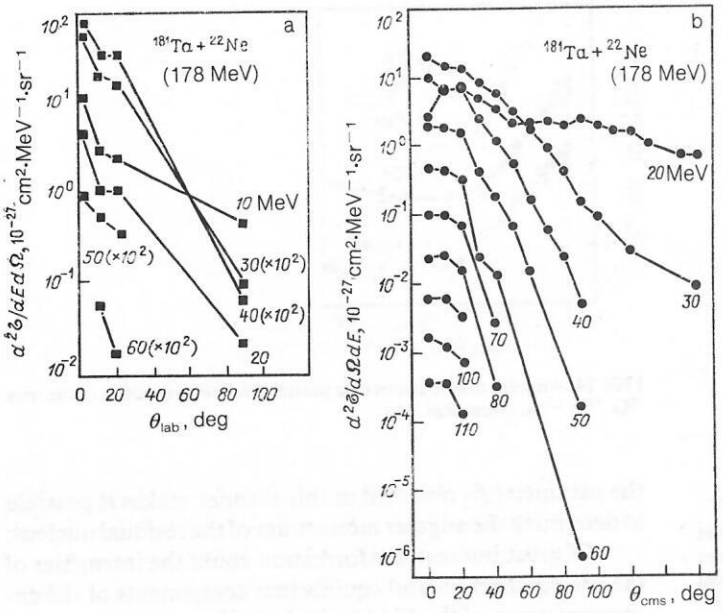

FIG. 15. Differential angular distribution of light particles for different energies: a) protons; b) α particles.

time in reactions with the heavier ions ^{20}Ne, ^{56}Fe, ^{63}Cu, ^{86}Kr, ^{132}Xe (Refs. 34, 45, 48, 49, and 109) did not reveal high-energy neutrons. In these studies, the angular and energy distributions of the neutrons could be described by assuming their equilibrium emission from fragments accelerated in the Coulomb field.

Recently, however, in reactions with accelerated neon ions, the emission of high-energy neutrons has been observed, first in Ref. 50 in the ^{181}Ta + ^{20}Ne reaction, and then in the ^{150}Nd + ^{20}Ne reaction[51] and the ^{165}Ho + ^{20}Ne reaction.[52] In Refs. 33, 53, and 54, in which oxygen and lithium ions were used as projectiles, the emission of such neutrons was also detected.

Thus, in the majority of studies made using accelerated heavy ions with mass $A_p \geqslant 56$ and energy 7–10 MeV/nucleon the emission of high-energy neutrons has not been observed, whereas for ions with $A_p \leqslant 20$ it has been. It can be assumed that this effect can be explained by the excess of the energy above the Coulomb barrier of the reaction $[\varepsilon = (E_p - V_{Co})/A_p]$, which in the case of heavy ions with mass $A_p \geqslant 56$ is 1–4 MeV/nucleon but in the case of the lighter ions is 5–8 MeV/nucleon. Thus, in Ref. 55, in which the ^{160}Er + ^{86}Kr reaction $[(E - V_{Co})/A_p = 7.5$ MeV/nucleon] was studied, the emission of high-energy neutrons was observed. All this indicates the necessity of accumulating experimental information with the aim of clarifying the probability of occurrence of this process, this including information obtained in correlation experiments.

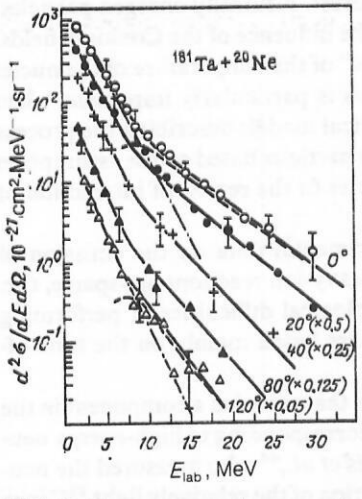

FIG. 16. Energy spectra of neutrons from the ^{181}Ta + ^{20}Ne reaction[56] at different angles. For the angles 0–120° the equilibrium and nonequilibrium components are separated.

In Ref. 56, a detailed investigation was made of the energy spectra of neutrons in the ^{181}Ta + ^{12}C and ^{181}Ta + ^{20}Ne reactions at ion energies around 9 MeV/nucleon. These same reactions have been well studied from the point of view of the emission of high-energy particles, including protons.[2,3,24] Figure 16 shows the energy spectra of the neutrons measured in Ref. 56 at angles from 0 to 120° in the laboratory system for the ^{181}Ta + ^{20}Ne reaction. The shape of the spectrum indicates the presence of two neutron components characterized by quite different slopes. If the slope of the spectrum is associated with a temperature, then the first component, which has a lower temperature, can be attributed to equilibrium emission of neutrons, whereas the second component can be attributed to nonequilibrium emission. With increasing angle, the temperature of the nonequilibrium part of the spectrum and its intensity decrease, as in the case of high-energy charged particles.[2,3] However, even for the angle 170° the temperature of the nonequilibrium part differs from the equilibrium value ($T = 1.7$ MeV). Comparison of the angular distributions of the neutrons for different sections of the energy spectrum, made in Ref. 56, showed that the angular distributions of the neutrons with energies above 10–15 MeV have a strong forward directionality, whereas the anisotropy of the angular distributions of the neutrons of lower energies is weak. This indicates once

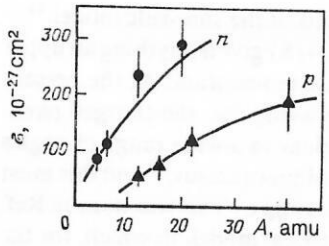

FIG. 17. Dependence of the n and p production cross sections on the mass of the bombarding ion.[56]

more that the neutrons with energies above 10 MeV are basically emitted in nonstatistical processes.

The values obtained for the total cross section for the emission of high-energy neutrons for different reactions but at the same value of $(E - V_{Co})/M$ indicate a possible dependence of the cross section on the mass of the bombarding ion up to $A_p = 40$. Figure 17 shows such a dependence for neutrons and protons. It can be seen that with increasing mass of the incident ion the cross section for the production of nonequilibrium neutrons and protons increases for the considered reactions. Unfortunately, information being unavailable, it is not possible to extend this dependence to the region of greater ion masses. It can be seen from the data in Fig. 17 that the probability of nonequilibrium emission of neutrons is greater than that for protons, although the dependence of the cross section on the ion mass is similar. Comparison of the yields of the hard components in the spectra of the protons and neutrons at different angles showed that at angle 0° the energy spectra of the protons and neutrons are nearly the same (Fig. 18).[56] For angles greater than 0°, the energy spectra of the protons and neutrons differ appreciably. The angular distributions of the protons are more anisotropic than those of the neutrons, and this may be explained by the influence of the Coulomb field of the system.

Thus, the characteristics of nonequilibrium neutrons produced in reactions with heavy ions to a large degree repeat those of the high-energy protons (see Sec. 2), and this can be taken as an indication of a similar mechanism of their production in heavy-ion reactions, as will be considered below.

5. ANGULAR MOMENTA OF NUCLEI FORMED IN REACTIONS WITH EMISSION OF HIGH-ENERGY CHARGED PARTICLES

The production of light charged particles can be associated with many reaction channels characterized by different impact parameters or entrance angular momentum (l^{ent}). However, what one determines directly in the experiments are the angular momenta I of the nuclei, the values of which can, in their turn, also give information about the reaction mechanism. A value $l^{ent} \ll l_{cr}$ or low spins I of the residual nucleus (l_{cr} is the critical angular momentum for formation of a compound nucleus) correspond to central collisions. Values $l^{ent} < l_{cr}$ or a broad distribution with respect to I in the residual nuclei indicate an evaporation nature of the charged-particle emission process.[57] A value $l^{ent} - l_{cr}$ and a narrow distribution of I values can correspond to breakup of the incident ion with subsequent capture by the target nucleus of part of the ion nucleus.[23] However, the three-body process with breakup of the incident nucleus in the field of the target nucleus does not lead to population of spins in the target nucleus ($I = 0$).[58] Thus, study of the populations of the spins of the residual nucleus and an estimate of l^{ent} in the channel corresponding to emission of fast charged particles (depending on the energy and species of the particle and on the energy and species of the bombarding ion) give information about the interaction of the colliding nuclei.

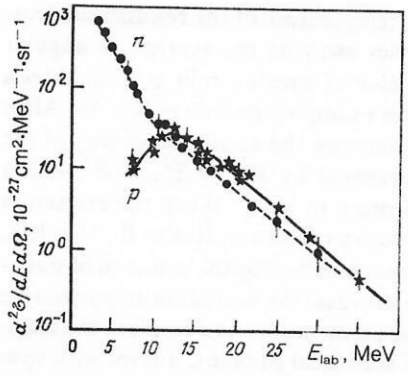

FIG. 18. Energy spectra of neutrons and protons measured at angle 0° in the $^{181}Ta + {}^{20}Ne$ reaction.

CONNECTION BETWEEN EXPERIMENTALLY MEASURED SPINS OF THE RESIDUAL NUCLEI AND THE ENTRANCE ANGULAR MOMENTA OF THE REACTION

After the emission of a charged particle, the residual nucleus, which is characterized by a certain excitation energy $E^*_{r.n}$ and angular momentum $l_{r.n}$, decays in accordance with the same laws as a compound nucleus, i.e., the de-excitation of the residual nucleus takes place mainly through the channels corresponding to evaporation of neutrons or secondary charged particles and through the fission channel.

The process of de-excitation of the residual nucleus is represented schematically in Fig. 19. Each ith neutron among the total number x of evaporated neutrons carries away on the average the energy $\Delta E^i_n = B^i_n + 2T_{r.n}$, where B^i_n is the binding energy of neutron i in the residual nucleus,

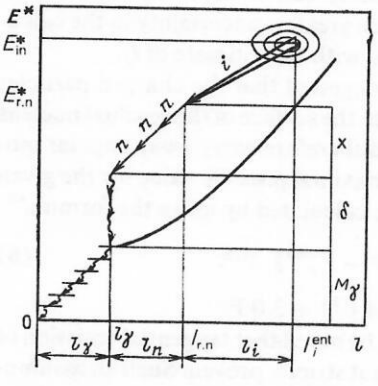

FIG. 19. Schematic representation of the emission of a charged particle from a compound system with subsequent de-excitation of the residual nucleus.

and $T_{r.n}$ is the nuclear temperature of the residual nucleus; each neutron also carries away on the average an angular momentum Δl_n, the value of which can be estimated by a calculation that uses, for example, the data of Ref. 59. After the evaporation of x neutrons, the excitation energy of the residual nucleus is decreased by $E^*_{xn} = \Sigma^x_{i=0} (B^i_n + 2T)$ and the angular momentum by $x\Delta l_n$. When the excitation energy of the residual nucleus becomes close to B^{i+1}_n or less, the de-excitation process continues by the emission of statistical γ photons, which decrease the excitation energy but do not carry away angular momentum. As a result of the emission of the cascade of statistical photons, a level with spin $l_{r.n} \simeq l_\gamma$ is populated in the residual nucleus, and subsequently the de-excitation process is terminated by a cascade of transitions along the yrast line and through levels of the ground-state rotational band. At the same time, all the angular momentum l_γ that remains after the emission of the last neutron is carried away from the residual nucleus. For $A_{r.n} > 200$, the fission channel of the residual nucleus becomes important after the emission of the charged particles. In this case, the values of $E_{r.n}$ and $l_{r.n}$ determine the angular anisotropy of the fission fragments detected in coincidence with charged particles.

The state of the residual nucleus with $l_{r.n}$ and $E^*_{r.n}$ is formed from a region of entrance states with respect to l^{ent} and E^*_{in} after the emission of a charged particle with energy E_i (Fig. 19). If it is assumed that the particle also carries away angular momentum l_i, it is possible to relate the mean value of the angular momentum l^{ent} in the entrance channel of the reaction corresponding to the emission of particle i to the mean values of the angular momenta carried away from the system in all stages of the de-excitation processes in an additive manner[60]:

$$l^{ent} = l_\gamma + l_n + l_i. \tag{6}$$

In the fission channel after the emission of the ith particle, l^{ent} can be obtained by means of the expression[61]

$$l^{ent} = l_f + l_i. \tag{7}$$

Here, l_f is the mean angular momentum of the fissioning residual nucleus.

In the expressions (6) and (7), l_γ and l_f can be determined experimentally and l_n can be obtained theoretically with a good accuracy. The greatest uncertainty in the calculation of l^{ent} is associated with the estimate of l_i.

In Ref. 62, it was suggested that the charged particles are emitted tangentially to the surface of the residual nucleus in the reaction plane and therefore carry away angular momentum l_i equal to the maximal possible value for the given energy; this value can be calculated by using the formula[60]

$$l_i = (r/\hbar)\,[2\mu\ (E_i^{cms} - V_i^{cms})\ ]^{1/2}, \tag{8}$$

where $r = 1.07(A_1^{1/3} + A_2^{1/3}) + 3.0$ F.

It should, however, be noted that tangential emission of the charged particles is not strictly proven. Such an assumption was adopted to obtain l_i^{ent} in the chosen reaction channel close to the critical angular momenta for the formation of a compound nucleus in the same reaction. This was done in accordance with the predictions of the sum-rule model.[23]

Thus, the expressions (6)–(8) give if anything an upper bound on the entrance angular momentum. At the present time there are grounds for believing that the charged particles are emitted from the nucleus in a wide range of angles relative to the surface of the residual nucleus,[63] and this must be taken into account in calculating l_i. This was done in Ref. 64 in the framework of a statistical model, in which, for the ^{180}Hf(^{12}C, αxn) reaction, a calculation was made of the mean value $\overline{\cos\theta}$ of the angle of emission of α particles from a composite nuclear system:

$$\overline{\cos\theta} = \frac{\int \cos\theta \rho\,(E_i\ |\mathbf{l}^{ent} + \mathbf{l}_i\,(\theta)|)\,d\theta}{\int \rho\,(E_i\ |\mathbf{l}^{ent} + \mathbf{l}_i\,(\theta)|)\,d\theta},$$

where $\rho(E_i\,|\mathbf{l}^{ent} + \mathbf{l}_i(\theta)|)$ is the level density of the residual nucleus, dependent on the sum of the vectors $\mathbf{l}^{ent}$ and $\mathbf{l}_i$.

Experimental methods of determining the angular momenta of the residual nuclei

The choice of the experimental method of determining the angular momenta carried away by the cascade of γ photons from the residual nucleus depends strongly on the properties of this nucleus. For even–even nuclei of the rare-earth region, for which the levels of rotational bands can be determined experimentally for spins greater than $20\hbar$, the best method is evidently the detection of the characteristic γ radiation by means of high-resolution γ spectrometers based on Ge or Ge(Li) detectors and the determination of the probabilities of level occupation. From the dependence of the relative probability of occupation of levels on their spin one determines the mean angular momentum $\overline{l}_\gamma$ and its variance, the relation $\overline{l}_\gamma = \overline{l}_{r.n}$ holding.

This method was used for the first time to investigate the incomplete fusion reaction ^{159}Tb(^{14}N, αxn)$^{169-x}$Yb at energy 95 MeV of the ions.[62] Alpha particles with energy greater than 33 MeV were detected by a ring detector placed at $\theta = 0°$. Gamma radiation in coincidence with α particles was observed by means of a Ge(Li) detector. For comparison, analogous measurements were made at angle $\theta = 180°$. Figure 20 shows the intensities of the γ transitions on the populated spin for the isotopes ^{165,166}Yb. The upper curve corresponds to the high-energy α particles detected at forward angles, and the lower curve to those detected at backward angles. From the dependence $Y(I)$ represented in the upper curve it is possible to establish the distribution of the angular momenta; this has a Gaussian shape with mean value $\overline{l}_\gamma = \overline{l} = 13\hbar$ and with FWHM of about $2\hbar$.[62] The lower curve corresponds to a broader distribution of states with a smaller mean angular momentum $\overline{l} \approx (9\text{–}10)\hbar$, and this corresponds more to an ordinary compound nucleus.

The method described above becomes invalid if one is studying residual nuclei with a complicated level scheme, for example, for odd-A nuclei, light or spherical nuclei, and nuclei in the transitional deformation region, i.e., it is invalid for the overwhelming majority of nuclei. To study the population of the spins of such nuclei, one can successfully use a method based on determination of the parameters of the distribution with respect to the multiplicity M_γ of the photons emitted by residual nuclei.[65,66]

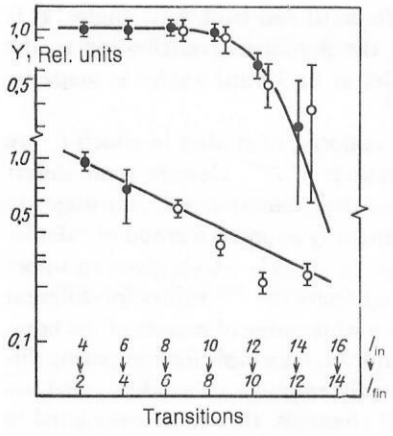

FIG. 20. Relative intensities of transitions between levels of the ground-state rotational bands of the nuclei ^{165}Yb (open circles) and ^{166}Yb (black circles) formed after emission of α particles in the ^{159}Tb + ^{14}N reaction. The upper and lower curves are obtained from measurements of α particles at forward and backward angles, respectively.

The method is based on measurement of the spectra of x or the γ radiation, and also particles for fragments that distinguish a particular reaction channel, in coincidence with photons of a γ de-excitation train of the residual nucleus. As photon detectors used to measure M_γ one employs NaI(Tl), CsI(Tl), BGO detectors, etc., which do not provide energy resolution of individual γ transitions but do make it possible to obtain an effectively constant efficiency Ω_γ of photon detection in a wide range of photon energies. This is important in the analysis of the experimental data.[65] The number N_γ of γ detectors used in this method can vary from one to several tens. If one detector is used in the experiment, it is possible to determine only the mean value $\langle M_\gamma \rangle$, i.e., the mean number of photons or their mean multiplicity. If several detectors are used, one can also measure σ_M, the standard deviation of the multiplicity distribution $\rho(M_\gamma)$, and S_M, the asymmetry parameter of the distribution $\rho(M_\gamma)$.[66] As a result of sorting the experimental data with respect to the response multiplicities of the γ detectors, we obtain, for example, the α-particle spectra Y_k corresponding to different numbers k of photons detected in coincidence with them. The experimental mean probabilities of k-fold coincidences are determined as

$$\langle P_k \rangle = \frac{Y_k}{SU}, \quad k = 0, \ldots, k_{\max},$$

where $SU = \sum_{k=0}^{k_{\max}} Y_k$. In the simplest case, in which a single γ detector is used in the experiment, $N_\gamma = k_{\max} = 1$, and $\langle M_\gamma \rangle$ can be obtained by means of the expression[67]

$$\langle M_\gamma \rangle = \frac{\ln \langle P_0 \rangle}{\ln (1 - \Omega_t)}.$$

Analyzing the results of experiments arranged in this manner, one can determine the angular momentum $\bar{l}_\gamma$ from the multiplicity $\langle M_\gamma \rangle$ by means of the expression

$$\bar{l}_\gamma = (\langle M_\gamma \rangle - \delta)\bar{f}_\gamma + I_0.$$

Here, I_0 is the difference between the spins of the initial and final states of the nuclei of the target and residual nucleus, respectively, δ is the number of statistical photons that do not carry away angular momentum, and $\bar{f}_\gamma$ is the mean angular momentum carried away by one photon.

This method was used in Ref. 60 to determine the values of $\langle M_\gamma \rangle$ for the channels $\alpha(3,4,5)n$ in the ^{159}Tb + ^{14}N reaction. It was shown for the first time in this study that for the channel corresponding to the emission of high-energy α particles a linear relationship exists between $\langle M_\gamma \rangle$ and $\bar{l}_\gamma$:

$$\langle M_\gamma \rangle = a\bar{l}_\alpha + b, \quad a < 0;$$

for the $\alpha 3n$ channel $\langle M_\gamma \rangle = -(0.77 \pm 0.22)\bar{l}_\alpha + (27.2 \pm 4.2)$; for the $\alpha 4n$ channel $\langle M_\gamma \rangle = -(0.73 \pm 0.27)\bar{l}_\alpha + (19.4 \pm 3.6)$.

Identification of the reaction channel using Ge detectors of x-ray radiation significantly raises the sensitivity of the experimental method.[68] This method of identifying the channel was used to measure $\langle M_\gamma \rangle$ for nuclei in the translational region of deformation.[63]

According to the data of Ref. 69, the succession of γ transitions in the de-excitation of residual nuclei in the transitional deformation region corresponds to several highly converted $M1$ transitions, as a result of which several x-ray photons with mean multiplicity $\langle M_x \rangle$ must be emitted in a single process of decay of the nucleus. Therefore, the calculation of the mean value of l_γ must be made with allowance for $\langle M_x \rangle$,[63] i.e.,

$$\bar{l}_\gamma = (\langle M_\gamma \rangle - \delta)\bar{f}_\gamma + \langle M_x \rangle + I_0.$$

For heavy residual nuclei there is a high probability of fission after emission of a high-energy particle. Analysis of data on the angular distribution of the fission fragments can also give information about the angular momentum l_f of the fissioning residual nuclei.[61,70] For example, the ^{209}Bi + ^{14}N reaction was investigated in Ref. 61 at ion energy 115 MeV. The angular distribution of the fission fragments in coincidence with α particles was measured in the reaction plane and out of it, and the angular momentum of the fissioning residual nuclei was determined. The method of determining the angular momenta in experiments arranged in this way is described in Ref. 71.

It should be noted that to detect light particles that precede fission of the residual nucleus at angle $\theta = 0°$ without identification of the reaction plane, it is possible to use the ordinary expressions relating the yield of fragments to their detection angle and the value of l_f.[72]

Population of rotational levels of the residual nucleus and entrance angular momenta in reactions with emission of high-energy particles

Several publications have given experimental data on the population of spins of the residual nuclei or measurement of the parameters of the M_γ distribution, i.e., the determination of the values of l_γ in the p, α, Li, etc., emission channels. As was noted in Sec. 2, many processes can contribute to an individually considered section of the inclusive spectrum. This is also true of a particular process—incomplete fusion reactions. For example, the channels $\alpha 3n$, $\alpha 4n$, and $\alpha 5n$ make comparable contributions to the spectrum of α particles at angle $\theta = 21.6°$ in the ^{14}N + ^{159}Tb reaction

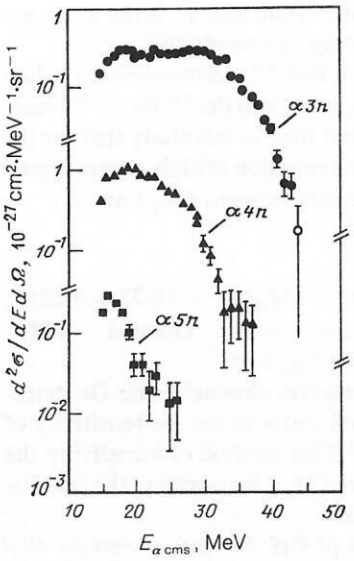

FIG. 21. Spectra of α particles measured at angle 21.6° in the laboratory system in the ^{159}Tb + ^{14}N reaction at energy 95 MeV of the nitrogen ions for the $\alpha 3n$, $\alpha 4n$, and $\alpha 5n$ de-excitation channels of the residual nucleus.

(Fig. 21).[60] It can be seen from Fig. 21 that to smaller values of x in the channel αxn there corresponds a broader spectrum of α particles, whereas to larger values of x there corresponds a narrow energy spectrum of the α particles with a maximum at energy E_α close to and even slightly less than the exit Coulomb barrier ($V_\alpha^{\mathrm{cms}} = 18.8$ MeV), this corresponding more probably to the evaporation emission mechanism.

It is therefore of interest to compare the values of l_γ (and $\langle M_\gamma \rangle$) for the different channels ixn for different energies of the particles at forward and backward angles. It is generally assumed that the dominant contribution to the yield of charged particles at backward angles is made by evaporation processes.[62]

The authors of the majority of studies in which l_γ are measured also give estimates of l^{ent}. Despite some differences in the approaches to the estimation of l_n, the majority of studies employ the generally adopted method of calculation [see the expressions (6)–(8)], which gives an upper bound for l^{ent}. One can compare the l^{ent} values for different reaction channels ixn in a wide range of masses of the bombarding ions and target nuclei. As a basis for comparing different reactions, one usually employs a "window" with respect to l for individual channels, this being calculated in accordance with the sum-rule model.[23,58] For the pxn and αxn channels, such a basis is frequently taken to be the critical angular momentum of complete fusion for the same reaction.

As was noted in Ref. 62, the region of entrance states with respect to l for the ^{159}Tb(^{14}N$\alpha 3n$) reaction is a narrow, $\sigma_M \sim 1\hbar$, Gaussian distribution for α particles emitted forward with angular momentum close to the critical angular momentum, $l^{\mathrm{ent}} \approx 40\hbar$ ($l_{\mathrm{cr}} = 37\hbar$). It was shown that α particles observed at backward angles correspond to a broader l^{ent} distribution, close to the l distribution in the fusion channel with a smaller value of $\bar{l}^{\mathrm{ent}}$.

In Ref. 60, the dependence of $\langle M_\gamma \rangle$ on E_α is given for the same reaction for different incomplete-fusion channels ($\alpha 3n$, $\alpha 4n$, and $\alpha 5n$) for the angle $\theta = 21.6°$ (Table V). Under the assumption $\bar{l}_\gamma = \langle M_\gamma \rangle \bar{f}_\gamma$, where $\bar{f}_\gamma$ is the mean angular momentum carried away by a single photon, and $\Delta l_n = 2\hbar$, values of $\bar{l}^{\mathrm{ent}}$ were obtained: $\bar{l}^{\mathrm{ent}}_{\alpha 3n} \approx 44\hbar$ and $\bar{l}^{\mathrm{ent}}_{\alpha 4n} \approx 40\hbar$, to within the errors of the experiment these being

TABLE V. Mean multiplicities $\langle M_\gamma \rangle$ of γ photons for the ^{159}Tb(^{14}N, αxn)$^{169-x}$Yb reaction at energy 95 MeV of the nitrogen ions as a function of the energy E_α.

Reaction channel	$E_{\alpha\,\mathrm{cms}}$, MeV		$\langle M_\gamma \rangle$
	Range	Mean value	
$\alpha 3n$	14.4—16.0	15.5	12.0±2.6
	16.0—19.0	17.5	12.2±1.2
	19.0—22.0	20.5	12.5±1.1
	22.0—25.0	23.5	13.1±1.0
	25.0—28.0	26.5	14.5±0.8
	28.0—31.0	29.5	14.1±0.7
	31.0—34.0	32.3	12.7±0.7
	34.0—37.0	35.2	11.3±0.9
	37.0—40.0	38.1	10.3±1.4
	40.0—43.0	41.0	7.5±2.8
	Complete energy range		13.0±0.4
$\alpha 4n$	14.4—16.0	15.5	15.6±1.6
	16.0—19.0	17.5	14.5±0.7
	19.0—22.0	20.4	11.6±0.6
	22.0—25.0	23.3	11.1±0.6
	25.0—28.0	26.2	8.2±0.8
	28.0—31.0	29.1	8.8±1.5
	Complete energy range		12.0±0.4
$\alpha 5n$	14.0—16.0	15.4	12.0±1.4
	16.0—18.0	17.0	10.5±1.1
	18.0—20.0	18.8	11.9±1.8
	20.0—22.0	20.7	10.2±3.2
	Complete energy range		11.3±0.8

TABLE VI. Mean multiplicity $\langle M_\gamma \rangle$ of γ photons as a function of the energy of α particles measured at angle 45° in the $^{20}Ne + {}^{150}Nd$ reaction at energy 175 MeV of the neon ions.

Exit reaction channel	$\langle M_\gamma \rangle$			
	Range of energy E_α, MeV			
	5.8–18.8	18.8–31.8	31.8–44.8	44.8–57.8
$^{160}Er + 6n$	22.0	23.5	26.5	25.0
$^{159}Er + 7n$	18.4	24.1	24.9	19.2
$^{158}Er + 8n$	24.3	24.3	21.8	18.7
$^{157}Er + 9n$	22.0	20.2	21.6	18.7

independent of E_α in the region $22 \leqslant E_\alpha \leqslant 40$ MeV and close to the critical angular momentum for the complete-fusion channel in the same reaction ($l_{cr} = 37\hbar$). For the $\alpha 3n$ channel, $\langle M_\gamma \rangle$ is observed to rise with increasing E_α up to the energy $E_\alpha \approx 28$ MeV, after which there is a monotonic decrease. For the $\alpha 4n$ and $\alpha 5n$ channels, such a rise is not observed. Moreover, for the $\alpha 5n$ channel $\langle M_\gamma \rangle$ does not depend on E_α. This circumstance is in good agreement with the data of Ref. 45, in which for the $^{158}Gd(^{12}C, \alpha xn)$ and $^{150}Nd(^{20}Ne, \alpha xn)$ reactions constancy of $\langle M_\gamma \rangle$ as a function of E_α is observed for most values of x for both reactions with different-mass heavy ions leading to the formation of the same residual nuclei (Table VI). The fact that $\langle M_\gamma \rangle$ does not depend on E_α can, as was noted in Ref. 60, be interpreted as a characteristic property of the evaporation of equilibrium α particles.

It was concluded in Ref. 73 that the structure of the residual nucleus has a dominant influence on the process of level population in the α-particle emission channel. This study found (Table VII) the same population of spins of the residual nucleus ^{164}Yb formed in three reactions with different masses of the incident ions; moreover, a rotational band was observed only up to relatively low spins ($I \sim 8^+$), despite the fact that the maximal angular momenta in these reactions differed very strongly. When the energy of the ^{20}Ne ions was increased to 151 MeV, the populated spin was not observed to increase, whereas the maximal angular momentum of the compound nucleus increase to $60\hbar$.

On the basis of a comparison of the experimental values of $\langle M_\gamma \rangle$ for the channels corresponding to the emission of high-energy p and α with $E_p > 20$ MeV and $E_\alpha > 60$ MeV in the $^{60}Ni + {}^{12}C$ reaction for $E_{^{12}C} = 194$ and 136 MeV with a calculation for the complete-fusion reaction and deep inelastic collisions, it was concluded in Ref. 74 that the dominant mechanism of these reactions is most probably one of evaporation from a compound system.

A decrease of $\langle M_\gamma \rangle$ with increasing mass (charge) of the emitted particle was observed in Ref. 75 (Table VIII). The same experiments measured the higher moments σ_M and S_M of the multiplicity distribution, indicating a Gaussian distribution $\rho(M_\gamma)$ with a small FWHM of about (8–14)$\hbar$. With allowance for the angular momentum carried away by the particle, values of $\overline{l}_{ixn}^{ent}$ for the channels (α, 2α, 3α, C)xn in good agreement with the position of the l windows were obtained.[25,58]

The values of l^{ent} obtained for the proton-emission channel in the $^{154}Sm + {}^{14}N$ reaction at ion energy 154 MeV agree well with the position of the l windows.[76] Good agree-

TABLE VII. Relative intensities of γ transitions between levels of the ground-state rotational bands in the residual nuclei as measured in $\gamma\alpha$ collisions.

Reaction	E_p, MeV	E_α, MeV	Residual nucleus	Transitions in residual nucleus		
				4–2	6–4	8–6
$^{159}Tb + {}^{10}B$	75	35—41	^{162}Er	0,97	1,0	0,91
$^{154}Sm + {}^{12}C$	85	28—33	^{158}Dy	1,01	1,0	0,94
$^{154}Sm + {}^{12}C$	109	42—56	^{158}Dy	0,89	1,0	0,99
$^{159}Tb + {}^{14}N$	115	35—39	^{164}Yb	0,98	1,0	0,94
$^{153}Eu + {}^{19}F$	112	23—29	^{164}Yb	1,0	1,07	0,92
$^{152}Sm + {}^{20}Ne$	119	23—27	^{164}Yb	1,03	1,0	1,07
$^{152}Sm + {}^{20}Ne$	151	24—31	^{162}Yb	1,0	0,86	0,73

Reaction	Transitions in residual nucleus						
	10–8	10–12	14–12	16–14	18–16	20–18	l_{max}, $\hbar$
$^{159}Tb + {}^{10}B$	0,73	0,47	0,18	0,18	—	—	12
$^{154}Sm + {}^{12}C$	0,91	0,80	0,68	0,46	0,31	0,18	21
$^{154}Sm + {}^{12}C$	1,06	0,74	0,95	0,42	0,32	—	25
$^{159}Tb + {}^{14}N$	0,85	0,74	0,63	0,36	0,20	—	34
$^{153}Eu + {}^{19}F$	0,94	0,73	0,57	0,37	0,28	0,23	38
$^{152}Sm + {}^{20}Ne$	0,81	0,51	0,42	0,19	—	—	40
$^{152}Sm + {}^{20}Ne$	0,36	0,19	—	—	—	—	60

TABLE VIII. Mean multiplicity $\langle M_\gamma \rangle$ and its standard deviation σ_M measured for different exit channels of the $^{154}Sm + {}^{16}O$ reaction at energy 153 MeV of the oxygen ions.

Exit reaction channel	$\langle M_\gamma \rangle$	σ_M
$^{159}Er + \alpha 7n$	21,5	5,9
$^{160}Er + \alpha 6n$	19,8	5,6
$^{156}Dy + 2\alpha 6n$	21,3	5
$^{157}Dy + 2\alpha 5n$	12,7	5
$^{154}Gd + Cxn$	11,0	4
$^{155}Gd + Cxn$	12,4	4
$^{156}Gd + Cxn$	10,3	4
$^{156}Gd + \alpha$	19,1	7.7
$^{156}Gd + C$	10,2	6.0

ment is observed for $\langle M_\gamma \rangle$ in the channels corresponding to emission of Li, Be, B, C, N, O, F, Ne in the $^{19}F + {}^{159}Tb$ reaction at 180 MeV.[117]

However, in many studies the data on l_i^{ent} differs strongly from the critical angular momentum. For example, in Ref. 61 in the $^{209}Bi(^{14}N, \alpha f)$ reaction at energy 115 MeV the value of $\overline{l}_{\alpha f}^{ent}$ is appreciably less [by (7–19)$\hbar$] than the value $l_{cr} \approx (50–53)\hbar$ for this reaction. The same result was obtained in Ref. 42 for the pf and αf channels in the ^{116}Sn, ^{154}Sm, ^{164}Dy, $^{197}Au(^{40}Ar, if)$ reactions at the energies 340, 272, 220 MeV.

If Ref. 15, the dependences of $\langle M_\gamma \rangle$ on E_α in the reactions on the target ^{124}Sn with ions ^{16}O, ^{19}F, and ^{70}Ne have, as was noted above, a characteristic rise up to energies 25 MeV, a monotonic decrease with increasing E_α for small x (the number of neutrons in the αxn channel), and a plateau at large x. In Ref. 15, estimates were obtained of $\overline{l}_{\alpha xn}^{ent}$ for "direct" and evaporation α particles. Comparing the ratios $l_{\alpha xn}^{ent}/l_{cr}$ for the two processes (direct and evaporation), the authors concluded that there is no sharp boundary with respect to l between these two processes. In addition, the values of l^{ent} are much smaller than the values of l_{cr} (on the average, $\overline{l}_{\alpha xn}^{ent}/l_{cr} \approx 0.45$), and this is in contradiction to the data given above from many studies (Refs. 45, 73, 75, and 76). The authors of Ref. 15 attribute this anomalously small

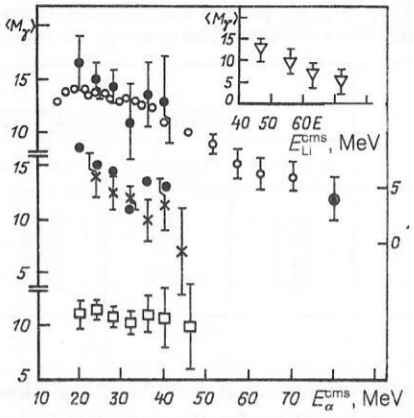

FIG. 22. Dependence of $\langle M_\gamma \rangle$ on the α-particle energy for different channels of the Ta + ^{22}Ne reaction. The open circles are for Ta(^{22}Ne, α), the black circles for Ta(^{22}Ne, αxn), the open squares for Ta(^{22}Ne, αf), and the crosses are the values of $\langle M_\gamma \rangle$ for the reaction $^{nat}Ir(^{12}C, \alpha xn)$. The insert shows the dependence of $\langle M_\gamma \rangle$ on the energy E_{Li} for the inclusive spectrum of the lithium nuclei in the Ta + ^{22}Ne reaction. All data correspond to the particle detection angle $\theta = 0°$.

value of $\overline{l}_{\alpha xn}^{ent}$ to the small deformation of the target nuclei. However, the incorrectness of such a conclusion is pointed out in Ref. 77. In the $^{118}Sn + {}^{12}C$ reaction the entrance angular momenta obtained in the pxn, αxn, ^8Bexn channels lie near l_{cr}, despite the fact that the ^{118}Sn nuclei are spherical. For these reactions, the values of $\langle M_\gamma \rangle$ and σ_M are given in Table IX.

The photon multiplicities in the αxn, Lixn, αf channels for the $^{181}Ta + {}^{22}Ne$ and $^{nat}Ir + {}^{12}C$ reactions were measured in Ref. 63. The data of these measurements are given in Fig. 22. In Ref. 63, the values of $\overline{l}_{\alpha xn}^{ent}$ were determined up to an energy of the α particles of about 80 MeV, which is only 25 MeV less than the kinematic limit for the $^{181}Ta + {}^{22}Ne$ reaction at energy 155 MeV of the ^{22}Ne ions (Fig. 23). The data indicate that in the α-particle emission channel the values of $\overline{l}^{ent}$ remain practically constant in a wide range of energies ($25 \leqslant E_\alpha < 80$ MeV) and do not depend on the combination of target nuclei (Ta, Ir) and bombarding ions (^{22}Ne, ^{12}C) leading to formation of the same compound nuclei (Tl). This is in disagreement with the pre-

TABLE IX. Mean multiplicity $\langle M_\gamma \rangle$ of γ photons and σ_M measured for the ixn channels of the $^{118}Sn + {}^{12}C$ reaction at energy 118 MeV of the bombarding ions.

Reaction	Transition		$\langle M_\gamma \rangle$	σ_M
	E_γ, keV	$I_{in}^\pi - I_{fin}^\pi$		
^{118}Sn (^{12}C, $\alpha 3n$) ^{123}Xe	456	$15/2^- — 11/2^-$	13,1	6.4
	617	$19/2^- — 15/2^-$	11.0	4,5
^{118}Sn (^{12}C, $\alpha 4n$) ^{122}Xe	331	$2^+ — 0^+$	14,2	7,7
	497	$4^+ — 2^+$	14,9	7,8
	638	$6^+ — 4^+$	14,5	7,8
	751	$8^+ — 6^+$	15,7	7,1
	822	$10^+ — 8^+$	14,3	5,6
^{118}Sn (^{12}C, $\alpha 5n$) ^{121}Xe	196	$7/2^- — 5/2^+$	12,1	8,1
	422	$15/2^- — 11/2^-$	12,6	8,2
	587	$19/2^- — 15/2^-$	10,8	7,8
^{118}Sn (^{12}C, $^8Be\ 2n$) ^{120}Te	560	$2^+ — 0^+$	8,2	6,3
	601	$4^+ — 2^+$	9,2	6,1
	615	$6^+ — 4^+$	9,1	5,6

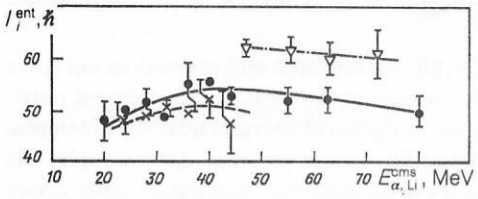

FIG. 23. Dependence on the energy of the charged particles of the entrance angular momenta for the following reactions: Ta(^{22}Ne, αxn) (black circles), Ir(^{12}C, αxn) (crosses), and Ta(^{22}Ne,Lixn) (open triangles).

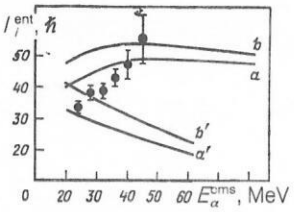

FIG. 25. Calculated values of the entrance angular momenta for different channels of the Ta + ^{22}Ne reaction as functions of the α-particle energy. The points are the experimental values of $l_{\alpha f}$.

dictions of the sum-rule model[23,58] for the position of the window with respect to the entrance angular momentum for the ^{181}Ta + ^{22}Ne reaction, $59 \leqslant \bar{l}^{ent}_{\alpha xn} \leqslant 63\hbar$, and for the Ir + ^{12}C reaction, $39 \leqslant \bar{l}^{ent}_{\alpha xn} \leqslant 43\hbar$. Moreover, it should be pointed out that the values of $\bar{l}^{ent}_{\alpha}$ for the ^{181}Ta + ^{22}Ne reaction lie significantly below the calculated value[78] of the critical angular momentum for formation of a compound nucleus, $l_{cr} = 66\hbar$, and somewhat above $l_{cr} = 44\hbar$ for the Ir + ^{12}C reaction.

In Ref. 63 measurements were made of the relative yields of the channels corresponding to fission and evaporation of neutrons and secondary charged particles accompanying the emission of high-energy α particles in the ^{181}Ta + ^{22}Ne reaction (Fig. 24). It was found that when $E_\alpha > 40$ MeV the neutron evaporation channel becomes dominant. Thus, the conclusion drawn in Ref. 79 is confirmed, namely, there is a connection between high-energy α particles and the yield of products in the αxn channel with a small value of x.[80]

From the experimental values of the ratio $W_f(\theta)$ of the fission-fragment yields measured in coincidence with α particles of different energies the residual angular momenta $\bar{l}_{\alpha f}$ of the fissioning Tl nuclei after emission of α particles were obtained as functions of E_α, the measurements being made

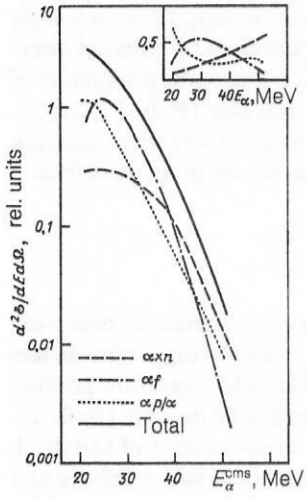

FIG. 24. Spectra of α particles in coincidence with products of the Ta + ^{22}Ne(155 MeV) reaction in different exit channels. The insert shows the relative yields of the various channels as functions of the energy E_α.

at angle $\theta = 0°$.[63]

On the basis of the data of Ref. 61 it can be assumed that the distribution of the entrance angular momenta for the ^{181}Ta + ^{22}Ne reaction is approximately the same for both channels (αxn and αf) of the reaction. On this basis one can calculate $\bar{l}^{ent}_{\alpha f}$, using the relation $\bar{l}_{\alpha f} = \bar{l}^{ent}_{\alpha f} - \bar{l}_{\alpha}$. The region of possible $l_{\alpha f}$ values for the case of tangentially emitted α particles is shown in Fig. 25 for $1 \leqslant \bar{f}_\gamma \leqslant 1.5$ (curves a' and b', respectively). On this basis it can be expected that the angular momenta of the residual nuclei after emission of α particles in the fission channel will lie in this region. However, this was found to hold only for $\bar{l}_{\alpha f}$ obtained from the experiment for the region $20 < E_\alpha < 30$ MeV, in which the αf channel is dominant. For larger values of E_α, corresponding to a relatively smaller contribution of the αf channel, the values of $\bar{l}_{\alpha f}$ appreciably exceed the expected values and become equal to the entrance angular momenta (curves a and b).

It was concluded from analysis of these data that the α particles are emitted at different angles to the surface of the residual nucleus, with the tangentially emitted particles carrying away the maximal possible angular momentum, while the radially emitted particles carry away a much smaller angular momentum. Thus, for the residual nucleus the relationship between the probabilities of fission and the evaporation of neutrons or secondary charged particles varies with the emission angle of the particle and its energy.

From this it also followed that for the αf channel the lifetime $\tau_{\alpha f}$ of the system before emission of an α particle detected at $\theta_\alpha = 0°$ must be an appreciable fraction (0.1–0.3) of the period of rotation $t_{rot} \sim 10^{-20}$ sec for $\bar{l}^{ent}_{\alpha} \approx 50\hbar$, this appreciably exceeding the typical time 10^{-22} sec of direct nuclear interactions.

The angular momenta in the reaction with ^{12}C ions on the ^{180} Hf target was studied in Ref. 64. In the α-particle emission channel, the exit angular momentum was found to be equal to $(38 \pm 2)\hbar$ in the region $20 \leqslant E_\alpha \leqslant 45$ MeV, which is significantly lower than the calculated value $l_{cr} = 45\hbar$.[78]

Comparison of the values of l^{ent} for reactions with ^{12}C ions on different targets using the same experimental method[63,64] showed that they do not depend on the mass of the bombarding particle.

In the framework of the same assumptions for analysis of the data, they were found to be very different for two reactions: $\bar{l}^{ent} = 38\hbar$ for ^{180}Hf + ^{12}C and $\bar{l}^{ent} = 50\hbar$ for Ir + ^{12}C. However, there have been studies, for example,

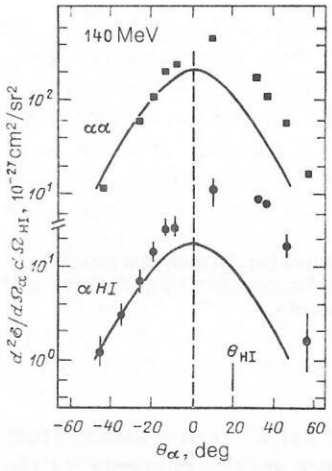

FIG. 26. Measured correlation functions in the plane of the reaction ^{159}Tb + ^{14}N [α, heavy ion (HI) and α, α]. The HI detector was at angle 20°.[96]

Ref. 81, in which the opposite conclusion is drawn—that the values of l^{ent} are correlated with the properties of the incident nucleus, namely, the binding energy in it of the ith particle.

Thus, the majority of authors are inclined to believe that the values of l^{ent} for the channels corresponding to the emission of charged particles are related to the properties of the compound nucleus. This is manifested especially for the ixn channels with relatively large values of x, to which there correspond relatively small values of E_α. For small values of x one observes a growth of $\langle M_\gamma \rangle$, and then, after movement of the maximum, a monotonic decrease. This feature in conjunction with the assumption of tangential emission leads to the obtaining of constant values of l^{ent}_{ixn}, independent of E_i.

Despite certain contradictions in the data given in the literature, it can be noted that in reactions with the emission of charged particles leading to the formation of residual nuclei the mean value of the populated spin $\overline{l}_\gamma$ of the residual nucleus decreases with increasing mass of the emitted particle. With allowance for the angular momentum carried away by the neutron cascade, the spin of the residual nucleus, $l_{\text{r.n}} = l_\gamma + x\Delta l_n$, is greater for larger values of x. Further, with allowance for the angular momentum carried away by a tangentially emitted particle, the values of $\overline{l}^{\text{ent}}_i$ increase with increasing mass of the ith particle.

No fundamental difference has been found for the mean values of the entrance angular momenta realized in the ixn and if channels.[61] In both cases they lie near the values l_{cr} for the formation of a compound nucleus.

Despite the rather large amount of information obtained on the angular momenta of the residual nuclei in incomplete-fusion reactions, it would be worth making experiments up to high energies of the charged particles even though this is undoubtedly a difficult problem requiring high sensitivity of the apparatus and long exposure times. Promising here are experiments with ions heavier than Ne and experiments to study reactions with different ion masses leading to the same residual nuclei, simultaneous study of the if and ixn channels in the same reaction, and also experiments in the region of large masses of the residual nuclei.[63]

Undoubtedly, all that has been said above does not solve the problem of the nature of the high-energy charged particles, particularly in the region of energies near the kinematic limit. Indeed, in the Ta + ^{22}Ne reaction, for example, the yield of α particles measured in coincidence with decay products of the residual nucleus is about 50% of the incluisve spectrum, whereas in the Ir + ^{12}C reaction it is only about 20%.[82] The remaining contribution in these reactions is made by α particles, which are evidently formed in other reaction channels and do not lead to the formation of residual nuclei.

Therefore, to establish the complete set of sources of charged particles it is also necessary to study the contribution of different processes and measure the correlations between the light particles and the reaction products.

6. RELATION BETWEEN THE REACTION CHANNEL WITH EMISSION OF HIGH-ENERGY PARTICLES AND OTHER REACTION CHANNELS

At an energy of the incident ion not much greater than the entrance Coulomb barrier the main reaction channels are the formation of a compound nucleus and quasielastic scattering. With increasing energy of the ion beam, there begins to be a greater probability of fast binary processes—incomplete-fusion reactions[62] and also deep inelastic reactions,[84] characterized by mass transfer between the interacting nuclei. As a rule, such reactions are accompanied by the emission of light charged particles and neutrons from the excited products. Particles of this kind can also be produced in incident-ion fragmentation processes[36,85] and other preequilibrium processes.[86]

In recent years, the experimentalist have made great efforts to elucidate these complex processes. To this end, they measure correlations between the light particles and the other reaction products and thus determine the contributions of the various processes to the cross section for the production of light particles measured in inclusive experiments. In accordance with various models, these processes are divided into two groups characterized by different interaction times—fast processes, which lead to the production of particles in the first stage of the reaction (Refs. 29, 36, 39, and 87), and relatively slow processes, in which the emission of the particles takes place from nuclei in an equilibrium state.

Particle–particle coincidences

The majority of correlation experiments for heavy-ion reactions have been made by measuring coincidences between a light particle (n, H, He) and a reaction product with mass near the mass of the projectile nucleus (Refs. 13, 60, 74, 88–91, and 93–102). In measurements of this kind, the detector of the projectilelike product had a definite and constant position during the time of the experiment. The angle θ of the position of this detector was taken to be either less than θ_{gr} (the angle of a grazing collision) if quasielastic conditions were studied, or somewhat greater than θ_{gr} if

deep inelastic interactions were investigated. The position of this detector and the direction of the beam determined the reaction plane. The light particles were measured by one mobile semiconductor ΔE–E detector or several detectors placed in the reaction plane at angle θ and outside the reaction plane at angle φ to it. In this manner, one can measure the correlation function (the curve of the intensity of coincidences as a function of the angles θ or φ), from the analysis of which the angular momentum of the emitter nucleus is determined. This method was used in Ref. 35 to determine the angular momenta of two complementary product nuclei of the $^{40}Ar + {}^{58}Ni$ reaction. The angular momenta obtained for different product nuclei were found to be 1.5 times greater than the angular momenta determined in experiments that measured the γ multiplicity.[103]

Analysis of the correlation function outside the reaction plane made it possible to identify a component that does not depend on the angle φ.[96,100] This is evidence for the production of high-energy particles in the first stage of the reaction.

Some conclusions about the reaction mechanism can also be drawn from analysis of the correlation function measured in the reaction plane. This curve (Fig. 26) has a maximum at the angle $\theta = 0°$. Depending on the combination of the colliding nuclei and their energy, the maxima of the correlation function can be displaced somewhat from 0°, and the slopes of the two sides of the maximum can also be different. In the correlation function, one usually separates the symmetric distribution around 0°, relating it directly to the mechanism of production of the high-energy particles. Analysis of the half-widths of the symmetric parts of the correlation functions in Refs. 91, 96, and 102 led to the conclusion that the processes of emission of high-energy particles are separated in time from the emission of the other reaction product measured in coincidence with these particles. It was shown that the high-energy α particle is emitted at an earlier stage of the reaction than the projectilelike particle. The α-particle emission time obtained in Refs. 91 and 102 was about 10^{-22} sec. The existence of the symmetric component of the correlation function, and also the similarity of the coincidence spectra and the inclusive spectra of the light particles enabled the authors of Refs. 91, 96, and 102 to determine the exclusive cross sections by simple addition of the cross sections of the inclusive particles measured in coincidence:

$$\frac{d^4\sigma\,[E_{\rm HI},\ \theta_{\rm HI},\ E_\alpha,\ \theta_\alpha]}{d\Omega_{\rm HI}\,dE_{\rm HI}\,d\Omega_\alpha\,dE_\alpha} = K\,\frac{d^2\sigma\,[E_{\rm HI},\ \theta_{\rm HI}]}{d\Omega_{\rm HI}\,dE_{\rm HI}}\,\frac{d^2\sigma\,[E_\alpha,\ \theta_\alpha]}{d\Omega_\alpha\,dE_\alpha},$$

where the subscript HI identifies variables corresponding to the heavy reaction product and the subscript α labels those belonging to the light particle. The cross sections obtained in the exclusive measurements depend strongly on the combination of the colliding nuclei and can differ by orders of magnitude.[96] The coefficient K remains practically constant and changes very slightly with increasing mass of the target nucleus. Therefore, K is a better indicator of the intensity of the pre-equilibrium component than the asymmetric part in the inclusive spectra.

The deviation of the maximum of the correlation functions from 0° and their asymmetric nature are explained by the emission of light particles from accelerated and excited reaction products. This is confirmed by analysis of the Lorentz-invariantly transformed cross sections as functions of the velocities of the products.[104] Figure 27 shows the velocity diagram for the $^{197}Au(^{36}Ar, S–\alpha)Au$ reaction. The arrows indicate the directions of emission of the primary products, and the circles around the arrows show the most probable velocities of particles emitted from the top of the barriers of the corresponding nuclei. It can be seen from the example shown in the figure that all the particles are grouped around velocities corresponding to the velocities of the projectile nucleus and the beam.

Comparison of the results of the correlation measurements with the predictions of various models that assume a definite reaction mechanism and also take into account the complete kinematics of the reactions showed (Refs. 34, 90, 99, and 106–111) that when heavy ions collide with nuclei at energies near the entrance Coulomb barriers the main sources of light particles, especially neutrons, are excited primary reaction products that evaporate particles in flight. However, these conclusions are not always unambiguous. Thus, after a more careful analysis of their data, made in Ref. 101, the authors of Ref. 90 drew attention to the existence of a group of α particles associated with the beam direction, whose origin cannot be explained by evaporation from primary products.

A direct indication of the existence of the emission of particles from projectile nuclei in quasielastic reactions was the observation of discrete lines in the spectra of α particles obtained in the rest frame of the emitter nucleus[95,96,100,113] and corresponding to levels of this nucleus.

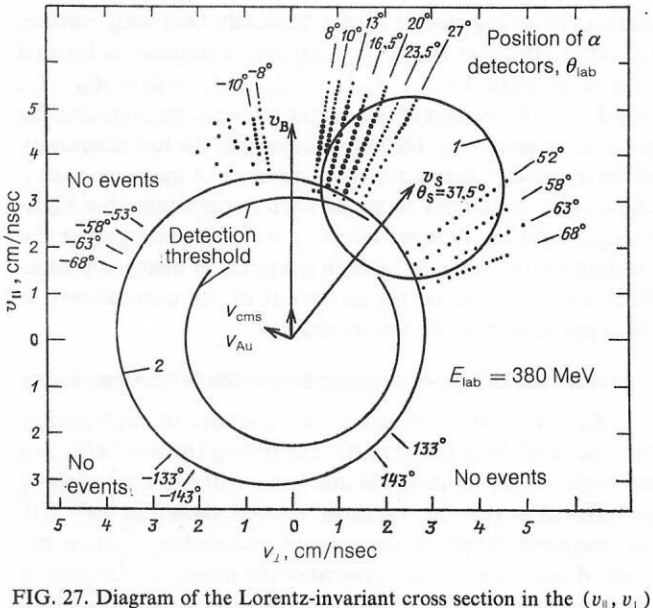

FIG. 27. Diagram of the Lorentz-invariant cross section in the $(v_\parallel, v_\perp)$ plane. The evaporation α particles must be grouped on a circle with center at the emission source. The radius of the circle corresponds to the Coulomb barrier between the two particles: circle 1 is the barrier for ^{32}S–^{197}Au, and circle 2 is the barrier for ^{197}Au–α. The detecting thresholds are indicated. The intensity of the point is proportional to $(1/P_\alpha)(d^3\sigma/d\Omega_{\rm HI}\,d\Omega_\alpha\,dE_\alpha)$ (from Ref. 104).

Of greatest interest is a component that cannot be explained by successive emission and which has become known as pre-equilibrium emission. As has been shown in many studies,[15,101,114] the yield of pre-equilibrium particles increases significantly with increasing energy of the bombarding ion. Correlation experiments with pre-equilibrium particles are extremely difficult because of the relatively small cross section for their production, especially at low energies of the bombarding particles. Therefore, the results of such experiments are not always unambiguous. Thus, in Ref. 87 a mechanism by which light particles are knocked out of the target by the beam was proposed. However, subsequent observation did not reveal a significant number of coincidences between light particles and products with Z near the atomic number of the nucleus of the bombarding ion.[104] In Refs. 62, 73, and 115, it was conjectured that pre-equilibrium particles are emitted as a result of mass transfer. In such an approach, it is assumed that in the first stage of the reaction the projectile breaks up into a light particle and a residue, which is then absorbed by the target nucleus. To investigate this mechanism, experiments were, as a rule, made in which coincidences of particles with γ photons of the residual nucleus were measured (Refs. 18, 23, 58, 69, 73, 118, and 119). The observation of characteristic γ transitions made it possible to determine precisely the final nucleus formed after emission of the light particle. These experiments were frequently accompanied by measurement of the multiplicity of the γ photons produced in the reaction, on the basis of which the angular momentum of the nuclei was determined. Experiments of this kind were considered in detail above. We shall here merely mention that in almost all the experiments in which coincidences of α particles with γ emission of the residual nuclei were studied it was shown that the mechanism of production of the light particles for weakly fissioning nuclei is of a basically two-body nature, i.e., after emission of the fast particle a nucleus is formed with mass equal to $A_{r.n} = A_M + A_p - A_i$, where A_M, A_p, and A_i are the masses of the target nucleus, the ion, and the particle, respectively. However, in view of the low sensitivity of the method of measuring coincidences of particles with γ photons, it is difficult to make such experiments for high-energy particles. A more effective way of investigating the mechanism of emission of such particles in heavy-ion reactions was found to be measurement of the correlations of these particles with fission fragments.

Coincidences of high-energy particles with fission fragments

Experiments to measure correlations of high-energy particles with fission fragments are among the most effective methods of investigating the mechanism of emission of these particles in heavy-ion reactions. As was shown in Ref. 120, the fragment emission angle in the laboratory system depends directly on the component of the moment of inertia of the fissioning nucleus parallel to the direction of the bombarding beam. Therefore, measurement of the emission angle of fragments in coincidence with a light particle makes it possible to determine the impact parameters for the given reaction and therefore to divide all the reaction products into groups depending on this parameter. In Ref. 120, a comparison was made of the angular distributions of fragments in coincidents with p, d, t, and α and a separation was made of events corresponding to central collisions in the $^{238}U + {}^{16}O$ system ($E = 315$ MeV) for $\theta \geqslant 160°$ and peripheral collisions ($\theta \leqslant 160°$). Comparison of the energy spectra of the particles for these two groups showed that they hardly differed, and the authors of Ref. 120 took this as an argument supporting the assumption of emission of the high-energy particles at an early stage in the development of the reaction—before fission. A similar conclusion was reached by the authors of Refs. 12 and 122–124, who also measured coincidences of p, d, t, and α particles with fragments produced by bombardment with ^{40}Ar ions of the targets ^{116}Sn, ^{154}Sm, ^{164}Dy, ^{197}Au, and ^{238}U. In these experiments, not only high-energy particles but also particles with energies corresponding to the exit Coulomb barrier and even somewhat lower were produced with relatively high probability.

In Ref. 124, which reports measurements of coincidences of α particles, with fission fragments of the nucleus ^{215}Fr produced after emission of α particles in the $^{197}Au + {}^{22}Ne$ reaction, it was shown that the kinetic-energy spectra of the fission fragments of the compound nucleus Ac and the Fr nuclei hardly differ. Measurement of the angle of inclination of the fission axis, determined by two fission-fragment detectors, relative to the direction of emission of the α particles did not reveal any significant change in the shape of the spectrum and yield of α particles, and this can be taken as evidence that the direction of emission of the α particles does not depend on the fission axis.

Combined study of the fission cross sections and the angular distributions of the fission fragments made with allowance for all decay channels of the nucleus formed after emission of an α particle is of great interest for investigating the limiting angular momenta realized in reactions of this kind. If the direction of emission of the α particle is close to the direction of the ion beam, then the distribution of the angular momenta of the compound nucleus becomes nearly isotropic in the plane perpendicular to the direction of the momentum of the recoil nucleus, which in the case of emission of high-energy α particles at angles $\leqslant 30°$ effectively coincides with the direction of the ion beam.[70] Therefore, the angular distributions of the fission fragments were analyzed by means of the usual expressions of the statistical model, except that the interval of initial states with respect to the excitation energy and angular momentum was related to the interval of averaging of the energies of the α particles measured in coincidence with the fission fragments. Bearing in mind that the main contribution to the emission of high-energy α particles is made by peripheral collisions, one could in this case expect that the angular anisotropy of the fission fragments would be somewhat greater than for the $^{197}Au(^{22}Ne, f)$ channel. The angular distributions of the fission fragments were measured in the $^{197}Au(^{22}Ne, f)$ and $^{197}Au(^{22}Ne, \alpha f)$ reactions (Fig. 28). Each angular distribution was normalized by the cross section for fission at angle 90° in the corresponding center-of-mass system of either the ^{219}Ac compound nucleus or the ^{215}Fr recoil nucleus. The

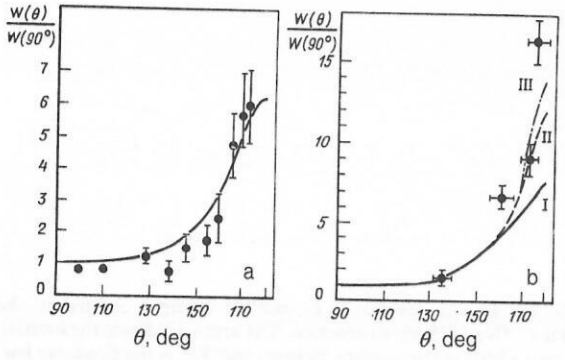

FIG. 28. Angular distribution of fission fragments: a) in the ^{197}Au(^{22}Ne, f) reaction; b) in the ^{197}Au(^{22}Ne, αf) reaction. The calculated dependences; I) $46 \leqslant l \leqslant 65$, $J_{sph}/J_{eff} = 1.2$; II) $46 \leqslant l \leqslant 65$, $J_{sph}/J_{eff} = 3$; III) $61 \leqslant l \leqslant 65$, $J_{sph}/J_{eff} = 3$.

angular distribution of the ^{219}Ac fission fragments calculated with allowance for the contributions of emission fission agrees well with the experimental distribution for $l_{cr} = 90\hbar$ and ratio $J_{sph}/J_{eff} = 1.2$. The angular anisotropy was 6.2. In the case of ^{215}Fr fission, the angular distribution is close to $1/\sin\theta$ with angular anisotropy $\geqslant 15$. The calculation was made in accordance with the formula

$$W(\theta) = \sum_{l=l_{min}}^{l_{max}} \sum_{i=0}^{m} \int_{E^*_{min}}^{E^*_{max}} (2l+1)\,\sigma_f(l_i, N_i, Z_i, E^*) \times I_0\left(\frac{l_i \sin^2\theta}{4K_{0i}^2(E^*)}\right) \exp\left(-\frac{l_i^2 \sin^2\theta}{4K_{0i}^2(E^*)}\right) dE^*.$$

The results of the calculation are given in Fig. 28.

It can be seen that the calculated angular anisotropy for liquid-drop values of the ratio, $J_{sph}/J_{eff} = 1.2$, is approximately equal to 7.5, and only the assumption of an anomalously large deformation of the nucleus, for which $J_{sph}/J_{eff} = 3$ (i.e., in the approximation of an ellipsoid of revolution with $R_{\parallel}/R_{\perp} = 3.6$), gives an anisotropy approximately equal to 12–13.

More plausible is the assumption that in the given reaction K_0^2 does not reach its equilibrium value but remains appreciably less, i.e., the fission process takes place rapidly and there is no thermal spreading of the orientation of the angular momentum relative to the direction of the fission axis. In this case, one can expect a shape of the angular distribution close to $1/\sin\theta$, and the mass distribution of the fragments must be broader than in the case of fission of a compound nucleus. However, despite the fact that the correlation experiments give the most complete information about the mechanism of emission of the high-energy particles and nuclei in heavy-ion reactions, their number so far is few, this being explained by the methodological difficulties of experiments of this kind. Therefore, in our view further understanding of the process of emission of high-energy particles must come about through accumulation of experimental data in correlation experiments.

7. POSSIBILITIES OF USING REACTIONS WITH EMISSION OF HIGH-ENERGY PARTICLES TO OBTAIN EXOTIC NUCLEI AND STUDY THEIR PROPERTIES

In reactions accompanied by the emission of high-energy particles it is possible to obtain nuclei with unusual properties (rapidly rotating, "cold," strongly deformed, and so forth); moreover, in this case the emitted particle is a good indicator of the properties of the residual nucleus. For example, by detecting α particles near the maximally possible energies in coincidence with the decay products of the residual nucleus, one can study the properties of these nuclei with almost no excitation energy. Confirmation of the formation of a weakly excited nucleus after the emission of a light particle can be provided by the excitation functions of the αxn reactions. If at high energies of the bombarding ions products associated with the channel $\alpha 0n$ or $\alpha 1n$ are observed, this indicates that the α particle has carried away the remaining fraction of the energy, and the residual nucleus is formed in a weakly excited state. Figure 1 shows the excitation functions of the ^{176}Lu(^{22}Ne, αxn)$^{194-x}$Au reaction for $x = 0$, 1, 2, 3 measured in Refs. 79 and 80. To take into account the contribution of the evaporation αxn, pxn, and xn channels of de-excitation of the compound nucleus and separate the channels associated with the emission of nonequilibrium α particles, the cross sections of the evaporation reactions were calculated in accordance with the formulas of the statistical theory. The results of these calculations are given in Fig. 1. It can be seen that once the energy of the ^{22}Ne ions is greater than 130 MeV the contribution of the evaporation channels falls rapidly, this being explained by the increasing role of processes associated with the emission of nonequilibrium α particles, while at energies $\geqslant 140$ MeV their contribution becomes dominant.

Thus, as follows from the experimental results in heavy-ion reactions accompanied by the emission of high-energy charged particles from the hydrogen isotopes to the beryllium isotopes, the emission of a particle predominantly in the forward direction is followed by the formation of a nucleus with mass less than the total mass of the nuclei of the ion and the target nuclei by the mass of the nucleus of the emitted particle and with excitation energy that depends on the energy carried away by the particle. Thus, reactions accompanied by the emission of a particle with energy at the kinematic limit lead to the formation of residual nuclei with zero excitation energy. A small difference between the limiting energy of the particle energy spectrum and the kinematic limit may be due to the angular momentum of the residual nucleus. This depends on the type of reaction and the emitted particle, and also on the bombarding energy. For example, in the case of the emission of Be nuclei the limiting energy of their energy spectrum practically reaches the kinematic limit, the cross section being relatively high (10^{-30} cm^2·MeV^{-1}·sr^{-1}; Fig. 29), and such reactions may be the most favorable ones for obtaining nuclei in the ground state.

Recently, several experimental attempts have been made[125] in reactions with the heavy targets ^{248}Gm, ^{254}Es, ^{249}Bk to obtain new spontaneously fissioning nuclei. In all the experiments made, the cross sections for the production of fermium isotopes and trans-fermium elements were found to be somewhat higher than expected as a result of many-nucleon transfer reactions. It could be that in this case there is a mechanism of formation of a heavy nucleus after emission of an energetic particle, for example, nuclei of beryllium

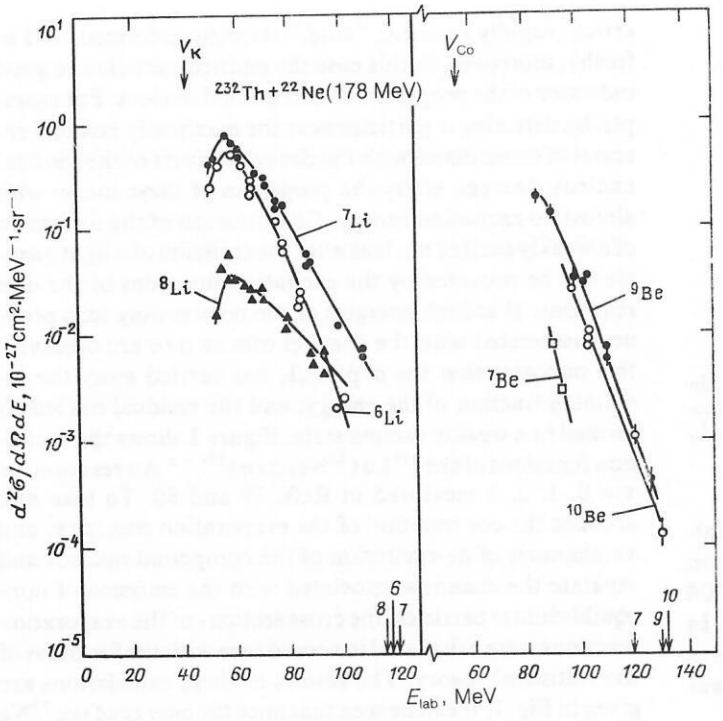

FIG. 29. Energy spectra of Li and Be isotopes emitted in the $^{232}Th + ^{22}Ne$ (178 MeV) reaction. The arrows indicate the limiting energies of the corresponding isotope, and V_{Co} is the Coulomb barrier in the exit channel.

or lithium. This question requires further experimental study.

In Ref. 126 an experiment was proposed that can unambiguously establish whether the production of heavy and superheavy nuclei in a reaction accompanied by the emission of high-energy charged particles is possible. It uses a magnetic spectrometer fixed at angle 0° relative to the beam. The light nucleus produced in the reaction and the heavy nucleus with mass $(A_M + A_p - A_i)$ corresponding to it enter the spectrometer and are observed by detectors placed at different positions in the focal plane. In the case of a two-particle reaction,the magnetic field of the spectrometer makes it possible to separate effectively the heavy nucleus and the beam, since the light nucleus, emitted in the first stage of the reaction, carries away a considerable fraction of the momentum.

If the reaction $^{248}Cm + ^{48}Ca$ is used, then by measuring the coincidence of high-energy α particles with the residual nucleus, which in this case must be the nucleus $^{292}114$, one can determine its properties even on the basis of a small number of events.

Reactions with the emission of high-energy particles may also be of great interest for studying the fission characteristics of heavy compound systems with $Z > 100$, in particular, for determining their fission barriers. Just as experiments are currently made to study low-energy fission of heavy nuclei in (d, pf) reactions[127] by observing coincidence of the fission fragments with high-energy particles in heavy-ion reactions, one can measure the fission characteristics of superheavy nuclei at different excitation energies determined by the energy of the emitted particle. Thus, one can obtain fissioning heavy nuclei with excitation energy $E^* \sim 5$–10 MeV by investigating the shape of the energy spectra of light particles in coincidence with fission fragments near the limiting energies of the particles, which to a large degree will be determined by the fissility of the nuclei, and one can obtain information about the fission barriers of such nulcei, including superheavy nuclei with $Z \sim 110$.

As was shown above, heavy-ion reactions lead with a relatively high probability to the production of neutron-rich isotopes of the lightest elements (He, Li, Be) with an energy corresponding to the maximally possible energy for the given reaction. In this case, the reaction products are weakly excited, and this is especially important for the synthesis of weakly bound nuclei near the nuclear stability limit, for example, ^9He, ^{10}He, ^{14}Be, ^{15}Be, ^{10}Li, ^{12}Li.

Figure 30 shows the energy spectrum of helium isotopes in the $^{232}Th + ^{11}B$ reaction, which was used in Ref. 128 to synthesize ^{10}He nuclei. The assumed cross section for the production of ^{10}He nuclei in this reaction, obtained by extrapolating the data on the cross sections of the light helium isotopes, must be $5 \cdot 10^{-30}$ cm^2/sr. However, the experimentally obtained upper limit for the production of ^{10}He nuclei in the $^{232}Th + ^{11}B$ reaction was $5 \cdot 10^{-34}$ cm^2/sr, indicating nuclear instability of ^{10}He.

Thus, reactions with the emission of high-energy particles induced by heavy ions can find and are already finding wide application for obtaining exotic nuclei and investigating their properties.

8. THEORETICAL MODELS OF THE EMISSION OF HIGH-ENERGY CHARGED PARTICLES

The large amount of data accumulated by the experimentalists on heavy-ion nuclear reactions accompanied by the emission of high-energy particles poses for theory the problem of explaining the complete set of these data or at least the main characteristics of these reactions, in particular:

a) the relative yield of the various particles and their

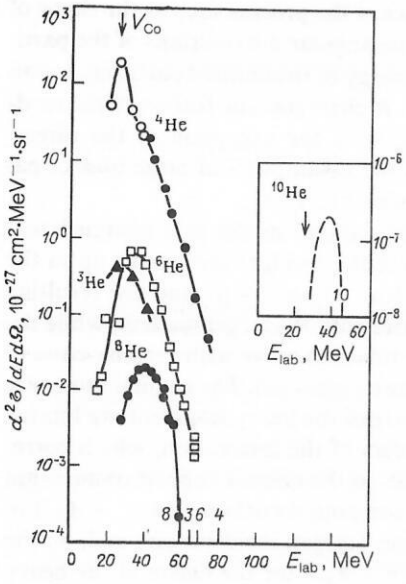

FIG. 30. Energy spectra of helium isotopes in the ^{232}Th + ^{11}B (89 MeV) reaction at angle $\theta = 20°$. The insert shows the assumed spectrum of ^{10}He (see the text).

multiplicities;

b) the shape of the energy spectra of the particles;

c) the shape of the angular distributions of the particles for different sections of the energy spectrum;

d) the dependence of the particle-emission cross section on the energy of the bombarding ion;

e) the distribution of the angular momenta between the products of reactions with the emission of light particles;

f) the behavior of the particle-reaction-product correlation functions.

The experimentally observed light particles can have different natures; they can be emitted from compound nuclei, fission fragments, the products of deep inelastic reactions, the bombarding nuclei, or the target nuclei and their fragments. Each of these cases is characterized by a certain time in which the reaction occurs, and this time can be experimentally measured. Another important characteristic of these reactions is the degree of dissipation of the kinetic energy of the bombarding nucleus and its redistribution between the reaction products; this can be estimated from the shape of the energy spectra of the particles of these products.

In this connection, to explain the set of data in a particular experiment, one uses one of the theoretical models containing assumptions about the reaction time or the degree of relaxation of the ion energy between the internal degrees of freedom of the reaction products.

Processes characterized by times longer than 10^{-21} sec and the establishment of thermal equilibrium in the reaction products are described by models of the statistical theory (Refs. 8, 83, 92, 121, and 129). On the basis of these models, programs have been created for calculating the reaction characteristics.[19,130–133] The possibilities of this approach are not restricted to describing the emission of light particles (n, p, α) but also explain the emission of heavier clusters. In the framework of these models, it is possible to analyze the low-energy part of the particle spectra. In conjunction with the Lorentz-invariant representation of the α-particle production cross sections, one can establish the sources of these particles and their relative contributions to the observed spectra.[135–138] A characteristic feature of these models is that they can be used in the case when the entrance angular momenta are less than l_{cr}.

Processes characterized by times of order 10^{-21} sec can be described by models of pre-equilibrium particle emission. One of these models is the exciton model, in which it is assumed that the process of kinetic-energy dissipation takes place through nucleon–nucleon collisions in the region of overlapping of the interacting nuclei. As a result of these collisions, some nucleons can become unbound and leave the system.[139,140] However, this model explains the emission of only neutrons and protons, describing their energy spectra. Only individual attempts have been made[141,142] to calculate the angular distributions of these particles in the framework of the exciton model. An important parameter of the theory is the number of excitons (n_0), which is usually set equal to the number of nucleons in the bombarding nucleus (A_p). However, for satisfactory description of the experimental data one usually requires a value $n_0 > A_p$, which, moreover, depends on the energy of the ions.[143] The exciton model also does not predict the nature of the distribution of the angular momenta between the reaction products.

Another method that describes the process of particle emission during a time $\leqslant 10^{-21}$ sec is the microscopic approach developed in Refs. 144 and 145 on the basis of time-dependent Hartree-Fock theory. In this approach, the time dependence of the wave function is calculated for each nucleon. One uses the adiabatic approximation, according to which the shape of the potential changes slowly compared with the motion of the nucleons in the potential well. Calculation in accordance with this model shows that for small impact parameters of the interaction, much less than l_{cr}, a "jet" of nucleons is formed along the direction of the motion of the incident ion. Their wave functions belong mainly to the bombarding nucleus. In this theoretical approach, one can describe well the growth in the cross section for the production of light particles at forward angles and the positions of the maxima of the energy spectra. At the same time, the calculated values of the light-particle emission cross sections are at a lower level than is observed experimentally.

For reactions characterized by times shorter than 10^{-21} sec, the model of prompt emission of particles has been proposed.[146,147] The basis of the model is that when the nuclei collide a window is formed through which the nucleons are transferred from nucleus to nucleus with velocity equal to the translational velocity of the nucleus and the Fermi velocity of the given nucleus. The total velocity of a nucleon can then be higher than is required to overcome the binding energy, and this particle leaves the system of interacting nuclei. The presence of the window and its size depend on the time and on the impact parameter of the collision $(0 < l > l_{gr})$. The shape of the energy spectra and the positions of their maxima calculated by this model are satisfactorily described. The particle-emission cross sections obtained by the calculation in accordance with this model are much smaller

than those observed experimentially.

The possibility of emission of high-energy particles is explained in the "hot spot" model.[26,27,86] The main assumption of this model is dissipation of a large fraction of the ion energy, the establishment of thermal equilibrium in the restricted region of contact of the colliding nuclei, and evaporation from this region of particles with energy corresponding to a high value of the temperature. It is assumed that with the passage of time this region expands, the temperature falls, and the process terminates with the establishment of thermodynamic equilibrium in the system as a whole. Thus, the model reflects the process of particle emission in the range of times $10^{-23} \leqslant t \leqslant 10^{-21}$ sec. When allowance is made for rotation of the compound system in the framework of this model, it is possible to obtain the dependence of the temperature of the emitting region on the angle at which the energy spectra of the particles are measured. Under a definite assumption about the impact parameter of the reaction, the mean time of α-particle emission in the $^{181}Ta + {}^{22}Ne$ reaction was found in Ref. 3 to be $7 \cdot 10^{-22}$ sec. To explain the energy spectra of particles measured at different angles, one usually makes the assumption of tangential emission from a hot spot, which is in disagreement with the basic hypothesis of the model of the statistical (isotropic) nature of their evaporation.[33] In Refs. 28 and 112, the assumption of tangential emission of the particles was replaced by taking into account the focusing effects of the refraction of the particles on the passage from the dense nuclear medium into the vacuum and distortion of the trajectory in the nucleon field of the system of colliding nuclei.

In Ref. 33, Awes *et al.* developed a model of a "moving source," which, like the hot-spot model [with the difference that the heated region (the source) is formed from nucleons of the ion and approximately the same number of nucleons of the target nucleus], moves in the direction of the bombarding ion with a velocity about half that of the ion after it has overcome the Coulomb barrier in the entrance channel. According to this model, the temperature does not depend on the angle of observation of the light particles. Kinematic analysis based on the diagrams of the Lorentz-invariant cross sections indicated the existence of two particle sources. The use of the moving-source model with allowance for precisely two sources significantly improves the agreement between the calculations and the experimental data. However, because of the large number of adjustable parameters in this model the physical meaning of the existence of these sources becomes unconvincing.[33]

The shortest nuclear reaction times are associated with direct processes. They are described by models that, depending on the approach, can be characterized as microscopic and phenomenological.

The microscopic approach, which has been used in a number of studies (Refs. 32, 39, 46, 47, and 134) to describe direct reactions with the emission of high-energy light particles, requires in the case of reactions with heavy ions significant simplifications to calculate the wave functions. Such simplifications generally have a reasonable physical basis (Refs. 39, 46, 47, and 134). In this connection, the final result of the calculations, which in the basic features correctly reflects characteristics of the process such as the shape of the energy spectrum, the angular distributions of the particles, and the limiting energy of the emitted particles, has an amount of uncertainty. A characteristic feature of the models of direct reactions, with the exception of the direct-knockout model,[116] is the assumption of large impact parameters of the interaction ($l \simeq l_{gr}$).

In the "incomplete-fusion" model it is assumed that when the nuclei interact the incident ion breaks up in the field of the target nucleus ($A_p = a + b$) and the resulting heavy fragment (b) fuses with the target nucleus, while the light fragment (a) continues to move with velocity close to the initial velocity of the incident ion. The angular momenta corresponding to capture of the heavy fragment are limited by the impact parameters of the interaction, which correspond, on the one hand, to the critical angular momentum for the formation of a compound nucleus, l_{cr} ($A_p + A_M$) in the original combination (target, incident ion) and, on the other hand, to the l_{cr} ($b + A_M$) for the fusion of the heavy fragment with the target nucleus.[58] Depending on the mass of the light emitted fragment, the lower and upper l limits of the reaction change, and there are thus formed the so-called angular-momentum windows in the entrance channel of the reaction. This model was developed in Ref. 18 and was called the "sum-rule" model. In this model the influence of the reaction energetics (Q_{gg}) and the rearrangement of the Coulomb energy is reflected, as in Ref. 105, in the calculation of the partial reaction cross sections for the different channels of fragmentation of the incident ion. The model of Ref. 18 was able to explain the predominant fusion of the heavy fragment with the target nucleus. Thus, the model correctly explains the yields of the various particles, including the enhanced yield of particles with the least separation energy (n, p, α), and also the values of the entrance angular momenta in the channels of light-particle emission, especially in reactions with light ions (up to $A_p \sim 16$). However, the model does not predict the shape of the energy spectra and the angular distributions of the emitted particles.

A further improvement of the model of Ref. 18 was made in Ref. 23. This modification made it possible to determine well the maxima of the energy spectra. The list of phenomenological models includes the fragmentation model of Ref. 36, the incomplete-fusion model of Ref. 58, and its modification in the form of the sum-rule model of Ref. 18.

Thus, the analysis of the experimental data made by means of these theoretical models has shown that at the present time it is not possible within the framework of one model to describe simultaneously all the main characteristics of reactions with the emission of high-energy particles, although individual characteristics can be satisfactorily described by particular models. Thus, to describe the shape of the energy spectra of the particles preference must apparently be given to the moving-source model,[33] while the explanation of the limiting energy of the particle spectra is most satisfactorily described in Ref. 39. The relative yields of the various particles and the corresponding values of the entrance angular momenta are well reproduced in the model of Ref. 17.

Further understanding of the mechanism of production of high-energy particles in heavy-ion reactions must proceed

through the accumulation of data of correlation experiments, extension of the range of masses and energies of the bombarding particles, and a further development of theoretical schemes capable of explaining the set of these experimental data.

[1)]Except for the case when $Z_{ion}Z_{targ} > 1500$, when various dynamical effects begin to have a significant influence on the formation of a compound nucleus.

[1]H. C. Britt and A. R. Quinton, Phys. Rev. **124**, 877 (1961).
[2]C. Borcea, E. Gierlik, A. M. Kalinin *et al.*, Nucl. Phys. **A391**, 520 (1982).
[3]C. Borcea, E. Gierlik, R. Kalpakchieva *et al.*, Nucl. Phys. **A415**, 169 (1984).
[4]J. Wilczyński, V. V. Volkov, and P. Dedowski, Yad. Fiz. **5**, 942 (1967) [Sov. J. Nucl. Phys. **5**, 672 (1967)].
[5]G. F. Gridnev, V. V. Volkov, and J. Wilcznynski, Nucl. Phys. **A142**, 385 (1970).
[6]J. Galim *et al.*, Nucl. Phys. **A159**, 461 (1970).
[7]R. Ost *et al.*, Nucl. Phys. **A265**, 142 (1976).
[8]M. Lefort, in: *Nuclear Spectroscopy and Nuclear Reactions with Heavy Ions, Proc. of the Intern. School of Physics Enrico Fermi 1974/Faraggi* (ed. Richi), North-Holland, Amsterdam (1976), p. 139.
[9]T. Sikkeland, E. L. Hainess, and V. E. Viola, Phys. Rev. **125**, 1350 (1962).
[10]E. Běták and V. D. Toneev, Fiz. Elem. Chastits At. Yadra **12**, 1432 (1981) [Sov. J. Part. Nucl. **12**, 574 (1981)].
[11]A. Kapustsik, V. P. Perelygin, S. P. Tret'yakova, and L. V. Ukraintseva, Yad. Fiz. **6**, 1142 (1967) [Sov. J. Nucl. Phys. **6**, 829 (1967)].
[12]D. Logan, M. Rajagopolan, M. S. Zisman *et al.*, Phys. Rev. C **22**, 104 (1980).
[13]R. Billerey, C. Cerruti, A. Chevarier *et al.*, Z. Phys. A **292**, 293 (1979).
[14]M. Rajagopolan, D. Logan, J. W. Ball *et al.*, Phys. Rev. C **25**, 2417 (1982).
[15]H. Tricoire, C. Gerschel, N. Perrin *et al.*, Z. Phys. A **306**, 127 (1982).
[16]H. Tricoire, Z. Phys. A **312**, 221 (1983).
[17]E. Gierlik, C. Borcea, and Yu. É. Penionzhkevich, *Mezhdunarodnaya shkola-seminar po fizike tyazhelykh ionov, Alushta, 14–21 aprelya, 1983 (International Seminar School on Heavy-Ion Physics, Alushta, 14–21 April, 1983);* Preprint D7-83-147 [in Russian], JINR, Dubna, p. 20.
[18]J. Wilczyński, K. Siwek-Wilczyńska, J. Van Driel *et al.*, Phys. Rev. Lett. **45**, 606 (1980).
[19]M. Blann and T. T. Komoto, Phys. Rev. C **24**, 426 (1981).
[20]J. M. Alexander, H. Delagrange, M. Rajagopolan, Z. Phys. A **307**, 149 (1982).
[21]A. G. Artukh, G. F. Gridnev, M. Gruszecki *et al.*, Preprint E7-81-355 [in English], JINR, Dubna (1981).
[22]E. Gierlik, A. M. Kalinin, R. Kalpakchieva *et al.*, Z. Phys. A **295**, 295 (1980); Yu. Ts. Oganessian, Yu. E. Penionzhkevich, E. Gierlik *et al.*, in: *Proc. of the Intern. Conf. on Nuclear Physics, Berkeley, 24–30 August,* 1980, LBL-1118, p. 491.
[23]J. Wilczyński, K. Siwek-Wilczyńska, J. Van Driel *et al.*, Nucl. Phys. **A373**, 109 (1982).
[24]C. Borcea, E. Gierlik, R. Kalpakchieva *et al.*, Nucl. Phys. **A351**, 312 (1981).
[25]H. Utsunomiya, T. Nomura, T. Inamura *et al.*, Nucl. Phys. **A334**, 127 (1980).
[26]R. Weiner and M. Weström, Nucl. Phys. **A286**, 282 (1977).
[27]R. Weiner and M. Weström, Phys. Rev. Lett. **34**, 1523 (1975).
[28]S. I. A. Garpman, D. Sperber, and M. Zielinska-Pfabe, Phys. Lett. **90B**, 53 (1980).
[29]R. V. Jolos and V. G. Kartavenko, Preprint R4-80-37 [in Russian], JINR, Dubna (1980); R. V. Jolos, S. P. Ivanova, and V. G. Kartavenko, Preprint R4-81238 [in Russian], JINR, Dubna (1981).
[30]T. C. Awes, G. K. Gelbke, B. B. Back *et al.*, Phys. Lett. **87B**, 43 (1979).
[31]T. C. Awes, G. K. Gelbke, G. Poggi *et al.*, Phys. Rev. Lett. **45**, 513 (1980).
[32]T. C. Awes, S. Saini, G. Poggi *et al.*, Phys. Rev. C **25**, 2361 (1982).
[33]T. C. Awes, G. Poggi, C. K. Gelbke *et al.*, Phys. Rev. C **24**, 89 (1981).
[34]D. Hilscher, J. R. Birkelund, A. D. Hoover *et al.*, Phys. Rev. C **20**, 576 (1979).
[35]R. Babinet, B. Gauvin, J. Girard *et al.*, Z. Phys. A **295**, 153 (1980).
[36]A. S. Goldhaber, Phys. Lett. **53B**, 306 (1974).
[37]J. R. Wu and I. Y. Lee, Phys. Rev. Lett. **45**, 8 (1980).
[38]D. K. Scott, Preprints MSUCL 355, 359 (1981).
[39]V. E. Bunakov and V. I. Zagrebaev, Izv. Akad. Nauk SSSR, Ser. Fiz. **47**, 2201 (1983).
[40]J. Galin, B. Gatty, D. Guerreau *et al.*, Phys. Rev. C **9**, 1113, 1126 (1974).
[41]H. Delagrange, D. Logan, M. F. Rivet *et al.*, Phys. Rev. Lett. **43**, 1490 (1979).
[42]D. Logan, H. Delagrange, M. F. Rivet *et al.*, Phys. Rev. C **22**, 1080 (1980).
[43]G. L. Catchen, M. Kaplan, J. M. Alexander, and M. F. Rivet, Phys. Rev. C **21**, 940 (1980).
[44]D. C. Sarantites *et al.*, Phys. Rev. C **18**, 774 (1978).
[45]L. Westerberg *et al.*, Phys. Rev. C **18**, 796 (1978).
[46]T. Udagawa and T. Tamura, Phys. Rev. Lett. **45**, 1311 (1980).
[47]T. Udagawa, D. Price, and T. Tamura, Phys. Lett. **116B**, 311 (1982).
[48]Y. Eyal *et al.*, Phys. Rev. Lett. **41**, 625 (1978).
[49]C. R. Gould *et al.*, Z. Phys. A **204**, 323 (1980).
[50]M. V. Blinov *et al.*, in: *Sb. annotatsiĭ Mezhd. simpoziuma po sintezu i svoĭstvam novykh élementov* (*Abstracts of the International Symposium on the Synthesis and Properties of New Elements*), Preprint D7-80-556 [in Russian], JINR, Dubna (1980), p. 64.
[51]A. Gavron *et al.*, Phys. Rev. C **27**, 450 (1983).
[52]E. Holub *et al.*, Phys. Rev. C **28**, 252 (1983).
[53]A. Gavron, F. L. Ferguson, F. E. Obenshain *et al.*, Phys. Rev. Lett. **46**, 8 (1981).
[54]O. V. Bochkarev *et al.*, in: *Voprosy atomnoĭ nauki i tekhniki. Seriya yadernykh konstant* (*Problems of Atomic Science and Technology. Series of Nuclear Constants*), No. 1 (40), TsNIIatominform, Moscow (1981), p. 28.
[55]I. Tserrya *et al.*, Phys. Rev. C **26**, 2509 (1982).
[56]É. M. Kozulin *et al.*, Preprint R7-85-31 [in Russian], JINR, Dubna (1985).
[57]J. H. Barker, J. R. Beene, M. L. Halbert *et al.*, Phys. Rev. Lett. **45**, 424 (1980).
[58]K. Siwek-Wilczyńska, E. H. Du Marchie von Voorthuysen, J. van Popta *et al.*, Phys. Rev. Lett. **42**, 1599 (1979); Nucl. Phys. **A330**, 150 (1979).
[59]J. M. Alexander and G. N. Simonoff, Phys. Rev. **133**, 93 (1964).
[60]T. Inamura, T. Kojima, T. Nomura *et al.*, Phys. Lett. **84B**, 71 (1979).
[61]H. Utsunomiya, T. Nomura, M. Ishihara *et al.*, Phys. Lett. **105B**, 135 (1981).
[62]T. Inamura, M. Ishihara, T. Fukuda, and T. Shimoda, Phys. Lett. **68B**, 51 (1977).
[63]V. V. Kamanin, A. Kugler, Yu. E. Penionzhkevich, and J. Rudiger, Nucl. Phys. **A431**, 545 (1984).
[64]V. V. Kamanin, A. Kugler, T. I. Mikhailova, and Yu. E. Penionzhkevich, in: *Intern. Symposium on Ion Beam Nuclear Spectroscopy, Debrecen, Hungary, May 14–18 (1984),* pp. 491–497.
[65]W. J. Ockels, Z. Phys. A **286**, 181 (1978).
[66]V. V. Kamanin, R. Kirkhbakh, A. Kugler *et al.*, Preprint 7–84-31 [in Russian], JINR, Dubna, (1984).
[67]B. F. Petrov, O. E. Kraft, and Yu. V. Naumov, Izv. Akad. Nauk SSSR, Ser. Fiz. **44**, 1970 (1980).
[68]H. W. Wilschut, R. K. Bhowmik, P. B. Goldhoorn *et al.*, Preprint KVI-383; Phys. Lett. **123B**, 173 (1983).
[69]H. J. Karwowsky, Phys. Rev. C **25**, 1355 (1982).
[70]C. Borcea, E. Gierlik, Yu. A. Muzychka, in: *Sb. Annotatsiĭ Mezhd. shkoly-seminara po fizike tyazhelykh ionov* (*Abstracts of the International Seminar School on Heavy-Ion Physics*), Preprint D7-83-147 [in Russian], JINR, Dubna (1983), pp. 25–26.
[71]P. Dyer *et al.*, Phys. Rev. Lett. **39**, 392 (1977); Nucl. Phys. **A322**, 205 (1979).
[72]R. Chaŭdhry, R. Vandenbosh, and J. R. Huizenga, Phys. Rev. **126**, 220 (1962).
[73]D. R. Zolnowski, H. Yamada, S. E. Cala *et al.*, Phys. Rev. Lett. **41**, 92 (1978).
[74]R. L. Robinson, R. L. Auble, I. Y. Lee *et al.*, Phys. Rev. C **24**, 2084 (1981).
[75]K. A. Geoffroy, D. G. Sarantites, M. L. Halbert *et al.*, Phys. Rev. Lett. **43**, 1303 (1979).
[76]J. Nyberg, A. Johnson, S. A. Hjorth *et al.*, *Abstract of the Contribution of the Intern. Symposium on Ion Beam Nuclear Spectroscopy, Debrecen, Hungary, May 14–18 (1984),* p. 68.
[77]S. E. Annell, A. Johnson, A. Kerek *et al.*, Phys. Lett. **129B**, 23 (1983).
[78]R. Schmidt, Fiz. Elem. Chastits At. Yadra **13**, 1203 (1982) [Sov. J. Part. Nucl. **13**, 501 (1982)].
[79]C. Borcea, E. Gierlik, R. Kalpakchieva *et al.*, Nucleonika, **26**, 1087

(1981).
[80]Kh. Brukhertzaĭfer, E. Langrok, Yu. A. Muzychka *et al.*, Yad. Fiz. **33**, 1453 (1981) [Sov. J. Nucl. Phys. **33**, 778 (1981)].
[81]J. R. Beene, M. L. Halbert, D. C. Hensley *et al.*, Phys. Rev. C **23**, 2463 (1981).
[82]J. Rudiger, "*Experimental study of the angular momenta of nuclei in heavy-ion reactions accompanied by the emission of light charged particles*" [in Russian], *Author's Abstract of Candidate's Dissertation*, Communication 7-84-539, JINR, Dubna (1984).
[83]T. D. Thomas, Ann. Rev. Nucl. Sci. **18**, 343 (1968).
[84]A. G. Artukh *et al.*, Nucl. Phys. **A215**, 91 (1973).
[85]V. K. Lukyanov and I. Z. Petkov, Nucl. Phys. **49**, 529 (1963).
[86]P. A. Gottschalk and M. Weström, Phys. Rev. Lett. **39**, 1250 (1977); Nucl. Phys. **A314**, 232 (1979); W. U. Schroder, in: *Proc. of the Intern. Symposium on Continuum Spectra of Heavy Ion Reactions, San Antonio, Texas, December 3–5 (1979).*
[87]D. H. E. Gross and J. Wilczyński, Phys. Lett. **67B**, 1 (1977).
[88]W. Kuhn, R. Albrecht, H. Damjantschitsch *et al.*, Z. Phys. A **298**, 95 (1980).
[89]J. W. Harris, T. M. Gormier, D. F. Geesman *et al.*, Phys. Rev. Lett. **38**, 1460 (1977).
[90]H. Ho, R. Albrecht, W. Dunnweber *et al.*, Z. Phys. A **283**, 235 (1977).
[91]R. K. Bhowmik, E. C. Pollaco, N. E. Sanderson *et al.*, Phys. Rev. Lett. **43**, 619 (1979).
[92]T. Ericson and V. M. Strutinski, Nucl. Phys. **8**, 284 (1958).
[93]M. B. Tsang, W. G. Lynch, R. J. Puigh *et al.*, Phys. Rev. C **23**, 1560 (1981).
[94]M. Bini, G. K. Gelbke, D. K. Scott *et al.*, Phys. Rev. C **22**, 1945 (1980).
[95]J. van Driel, S. Gonggrijp, R. V. F. Janssens *et al.*, Phys. Lett. **98B**, 351 (1981).
[96]R. K. Bhowmik, J. van Driel, H. Siemssen *et al.*, Nucl. Phys. **A390**, 117 (1982).
[97]A. Gamp, J. C. Jacmart, N. Poffe *et al.*, Phys. Lett. **74B**, 215 (1978).
[98]K. G. Young, D. C. Sarantites, J. R. Beene *et al.*, Phys. Rev. C **23**, 2479 (1981).
[99]Y. Eyal, A. Gavron, I. Tserruya *et al.*, Phys. Rev. C **21**, 1377 (1980).
[100]T. Fukuda, M. Ishihara, M. Tanaka *et al.*, Phys. Rev. C **25**, 2464 (1982).
[101]H. Ho, P. L. Gonthier, G. Y. Fan *et al.*, Phys. Rev. C **27**, 584 (1983).
[102]R. K. Bhowmik, E. S. Pollaco, N. E. Sanderson *et al.*, Nucl. Phys. **A363**, 516 (1981).
[103]A. Albrecht, B. B. Back, R. Bock *et al.*, in: *European Conf. on Nuclear Physics with Heavy Ions*, Caen (1976), p. 167.
[104]A. Gamp, M. Burgel, M. R. Clover *et al.*, Z. Phys. A **300**, 63 (1981).
[105]V. V. Volkov, Preprint R7-82-661 [in Russian], JINR, Dubna (1982).
[106]J. Peter, M. Berlanger, C. Ngo *et al.*, Z. Phys. A **283**, 413 (1977).
[107]D. Guerreau, BNL Report No. BNL-5115 (1979), p. 59.
[108]C. R. Gould, R. Bass, J. V. Czarnecki *et al.*, Z. Phys. A **284**, 353 (1978).
[109]B. Tamain, R. Checnik, H. Fuchs *et al.*, Nucl. Phys. **A330**, 253 (1979).
[110]G. R. Young, R. L. Ferguson, A. Gavron *et al.*, Phys. Rev. Lett. **45**, 1389 (1980).
[111]R. Billerey, C. Cerruti, A. Chevarier *et al.*, Z. Phys. A **284**, 319 (1978).
[112]W. W. Morison *et al.*, Phys. Lett. **93B**, 379 (1980).
[113]H. Homeyer, M. Burgel, M. Glover *et al.*, Phys. Rev. C **26**, 1335 (1982).
[114]C. Gerschel, Nucl. Phys. **A387**, 297 (1982).
[115]H. Yamada, D. R. Zolnowski, S. E. Cala *et al.*, Phys. Rev. Lett. **43**, 605 (1979).
[116]V. E. Bunakov and V. I. Zagrebaev, Z. Phys. A **304**, 231 (1982).
[117]R. H. Siemssen, Preprint KVI-399, Groningen, Netherlands (1982).
[118]C. Gerschel, N. Perrin, L. Valentin *et al.*, in: *Proc. of the Intern. Conf. on Nuclear Behavior*, Strasbourg (1980); J. Phys. C **10**, 239 (1980).
[119]V. V. Kamanin, Yu. Ts. Oganesyan, Yu. É. Penionzhkevich *et al.*, Preprint 7-81-726 [in Russian], JINR, Dubna (1981).
[120]P. Dyer, T. C. Awes, C. K. Gelbke *et al.*, Phys. Rev. Lett. **42**, 560 (1979).
[121]T. Ericson Adv. Phys. **9**, 425 (1960).
[122]M. Kildir, D. Logan, M. Kaplan *et al.*, Z. Phys. A **306**, 323 (1982).
[123]M. F. Rivet, D. Logan, J. M. Alexander *et al.*, Phys. Rev. C **25**, 2430 (1982).
[124]E. Gierlik, A. M. Kalinin, R. Kalpakchieva *et al.*, Yad. Fiz. **32**, 45 (1980) [Sov. J. Nucl. Phys. **32**, 23 (1980)].
[125]J. M. Nitschke, in: *Sb. annotatsiĭ Mezhd. simpoziuma po sintezu i svoĭstvam novykh élementov* (*Abstracts of the International Symposium on the Synthesis and Properties of New Elements*), Preprint 07-80-556 [in Russian], JINR, Dubna (1980), p. 28.
[126]A. V. Belozerov, A. M. Kalinin, Yu. Ts. Oganesyan, and Yu. É. Penionzhkevich, in: *Sb. annotatsiĭ. Soveshchanie po éksperimental'nym ustanovkam, U-400, Drezden (Abstracts of Papers at the Symposium on the Experimental U-400 Facilities, Dresden)*, Preprint 07-82–891 [in Russian], JINR, Dubna (1982), p. 40.
[127]H. C. Britt, D. C. Hoffman, J. van der Plicht *et al.*, Phys. Rev. C **30**, 559 (1984).
[128]Yu. Ts. Oganesyan, Yu. É. Penionzhkevich, E. Gierlik *et al.*, Pis'ma Zh. Eksp. Teor. Fiz. **36**, 104 (1982) [JETP Lett. **36**, 129 (1982)].
[129]M. Lefort, Rep. Prog. Phys. **39**, 129 (1976).
[130]M. Blann and J. Bisplinghoff, Preprint UCID-19614 (1982).
[131]J. R. Grover and J. Gilat, Report BNL 50 (1970), p. 246.
[132]J. Gomez del Campo, Phys. Rev. Lett. **36**, 1529 (1976); J. Gomez del Campo and R. Stokstad, Report ORNI-TM 7295.
[133]F. Puhlhofer, Nucl. Phys. **A280**, 267 (1977).
[134]C. V. Christov, I. J. Petkov, and I. I. Délchev, Trieste Report Ic/82/211 (1982).
[135]E. Duek, L. Kowalski, and J. Alexander, Preprint IPNO-DRE-82.20, Orsay.
[136]E. Duek, L. Kowalski, and J. Alexander, Comput. Phys. Commun. **34**, 395 (1985).
[137]E. Duek, L. Kowalski, M. Rajagopalan *et al.*, Z. Phys. A **307**, 221 (1982).
[138]E. Duek, L. Kowalski, M. Rajagopalan *et al.*, Z. Phys. A **307**, 237 (1982).
[139]M. Blann, Phys. Rev. C **23**, 205 (1981).
[140]T. Otsuka and K. Harada, Phys. Lett. **121B**, 106 (1983).
[141]J. M. Akkermans, H. Gruppelaar *et al.*, Phys. Rev. C **22**, 75 (1980).
[142]A. Chatterjee, Z. Phys. A **313**, 93 (1983).
[143]E. Holub *et al.*, Z. Phys. A **314**, 347 (1983).
[144]K. R. S. Devi *et al.*, Phys. Rev. C **24**, 2521 (1981).
[145]K. T. R. Davies, K. R. S. Devi, and R. M. Strayer, Preprint MAR-23 (1982).
[146]J. R. Bondorf, J. N. De, A. O. T. Karvinen *et al.*, Phys. Lett. **84B**, 162 (1979).
[147]J. P. Bondorf, J. N. De, and A. O. T. Karvinen, Nucl. Phys. **A333**, 285 (1980).

Translated by Julian B. Barbour